

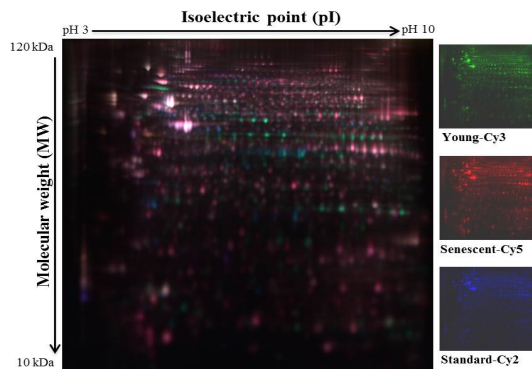


UNIVERSITA' DI NAPOLI FEDERICO II

**DOTTORATO DI RICERCA
BIOCHIMICA E BIOLOGIA CELLULARE E MOLECOLARE
XXVII CICLO**

Mariangela Succoio

*A proteomic approach for the identification of novel
direct targets of microRNA-494 and of novel
mediators of cellular senescence*



Academic Year 2013/2014



UNIVERSITA' DI NAPOLI FEDERICO II

**DOTTORATO DI RICERCA
BIOCHIMICA E BIOLOGIA CELLULARE E MOLECOLARE
XXVII CICLO**

*A proteomic approach for the identification of novel
direct targets of microRNA-494 and of novel
mediators of cellular senescence*

**Candidate
Mariangela Succio**

Tutor
Prof. Raffaella Faraonio

Coordinator
Prof. Paolo Arcari

Academic Year 2013/2014

Ringraziamenti e dediche

Al termine di questo mio percorso di studi desidero fortemente ringraziare tutte le persone che a vario titolo mi hanno accompagnato lungo questi tre anni di dottorato e senza le quali questo lavoro di tesi non sarebbe stato possibile.

Innanzitutto ringrazio la Prof.ssa Raffaella Faraonio per essersi sempre dimostrata disponibile a offrirmi il proprio preziosissimo contributo teorico e metodologico durante tutte le fasi del mio lavoro di ricerca nonché dritte che mi hanno consentito di crescere sia da un punto di vista professionale che personale.

Desidero ringraziare il Prof. Filiberto Cimino che per me costituirà sempre un modello di intelligenza, correttezza, amore per la ricerca e professionalità da perseguire nella vita e nel lavoro.

Con tutto il mio cuore ringrazio Marika per essermi sempre stata vicina in questi lunghi tre anni e non solo come collega di laboratorio ma come amica e senza la quale questo dottorato non sarebbe mai stato altrettanto prezioso.

Voglio, inoltre, ringraziare tutti i tesisti del laboratorio (Raffaele, Rocco, Ilaria e Roberta), la mia amica/dottoranda Raffaella Liccardo e gli altri colleghi con cui ho condiviso lezioni, impegni, preoccupazioni e frustrazioni, oltre che a idee e soddisfazioni.

Ringrazio i colleghi/collaboratori che hanno contribuito alla nostra attività di ricerca e hanno permesso di migliorare il presente lavoro di ricerca: Prof. Nicola Zambrano, Monica Vitale, Prof. Andrea Scalonì, Chiara d'Ambrosio, Fabiana Passaro e Marco Napolitano.

Un ringraziamento particolare a Marina, la mia amica del cuore e di studi, un grazie sincero e profondo per aver creduto in me quando tutti i miei obiettivi sembravano irraggiungibili, grazie per essermi stata sempre vicina e pronta a darmi saggi consigli nonostante i chilometri di distanza che ci hanno separato in questi anni.

Non posso dimenticare l'immenso debito di gratitudine verso i miei genitori, Stefania e Gennaro, i quali hanno sostenuto le scelte professionali più importanti della mia vita e non hanno mai mancato di incondizionato amore, ascolto e attenzione, spronandomi sempre ad andare avanti per la mia strada.

Ringrazio i miei fratelli a cui voglio un bene immenso, Martina, Gianfranco e Lorenzo per il loro amore e per avermi sempre sopportata durante questi anni nonostante i miei sbalzi d'umore. Ed infine ringrazio il mio futuro marito Gianni per essermi stato sempre vicino, per avermi supportato nei momenti di sconforto e per aver condiviso con me i momenti di difficoltà cercando sempre di confortarmi e rallegrarmi, tenendo fede al nostro amore.

Grazie!

Mariangela

Riassunto

Le cellule normali non si replicano all'infinito, piuttosto dopo un certo numero di divisioni, entrano in uno stato di arresto permanente della proliferazione definito senescenza cellulare.

La senescenza cellulare è accompagnata da una riprogrammazione del profilo di espressione genica, conseguente a modifiche dei meccanismi di regolazione che agiscono sia a livello trascrizionale che post-trascrizionale così come a livello epigenetico.

I microRNA (miRs) sono piccoli RNA non codificanti che svolgono un ruolo fondamentale nella regolazione negativa dell'espressione genica a livello post-trascrizionale. Essi riconoscono sequenze al 3'UTR e bloccano la traduzione o determinano la degradazione di RNA messaggeri.

Nel laboratorio in precedenza erano stati identificati 24 miRs (SAmiRs) up- o down-regolati nella senescenza cellulare di fibroblasti primari IMR90. Studi funzionali sui SAmiRs up-regolati avevano dimostrato che 5 di essi sono in grado di indurre un fenotipo di senescenza precoce quando iper-espressi in cellule giovani, in particolare, il miR-494 è quello che provoca il fenotipo senescente più marcato.

I nostri studi hanno perseguito due obiettivi fondamentali:

- i) studiare le vie regolatorie in cui è coinvolto il miR-494 attraverso l'identificazione dei suoi targets molecolari;
- ii) identificare nuovi mediatori/effettori comuni della senescenza cellulare indotta sia dall'accorciamento dei telomeri che provocata dallo stress ossidativo.

Per entrambi gli obiettivi, è stato scelto un approccio *high-throughput* di tipo proteomico utilizzando la tecnologia del 2D-DIGE (Two Dimensional-Difference Gel Electrophoresis) accoppiata alla Spettrometria di Massa (LC-MS/MS).

Nell'ambito del primo obiettivo, per individuare possibili targets del miR-494, abbiamo monitorato con il 2D-DIGE i cambiamenti a livello proteico conseguenti alla sua iper-espressione nelle cellule IMR90 giovani, considerando che esiste una relazione inversa tra livelli dei miRs e livelli proteici espressi dai loro targets. L'analisi 2D-DIGE ci

ha permesso di considerare circa 1500 spot proteici presenti in ambedue le condizioni. Tra questi, 102 spot proteici (38 up- e 64 down-regolati) sono risultati differenzialmente rappresentati nelle cellule trasfettate con il miR-494, comparate con cellule controllo trasfettate con un miR-scramble. Con la spettrometria di massa sono state identificate 172 specie proteiche differenti, di cui 121 presenti negli spots down-regolati. Un'analisi *in silico*, ha consentito di identificare tra queste, 26 putativi targets del miR-494, di cui 9 sono stati da noi selezionati per l'analisi funzionale. Con saggi di attività della luciferasi abbiamo dimostrato che quattro di essi (hnRNPA3, PDIA3, RAD23B, SYNCRIP/hnRNPA3) presentano siti di legame funzionali per il miR-494. Abbiamo anche dimostrato che l'espressione di hnRNPA3, PDIA3, RAD23B, SYNCRIP è diminuita oppure aumentata in condizioni di iper-espressione o inibizione del miR-494, rispettivamente. La ridotta espressione di tali proteine è stata anche ritrovata in altri modelli di senescenza cellulare. Abbiamo anche dimostrato che il silenziamento di hnRNPA3 o RAD23B in cellule giovani IMR90 induce un fenotipo senescente simile a quello indotto dall'over-espressione del miR-494, e mediato dall'attivazione del pathway di p53. Infine, altri risultati hanno dimostrato che il fenotipo senescente indotto dal miR-494 è prevenuto se nelle cellule è stato introdotto il gene hnRNPA3 oppure RAD23B.

L'altro aspetto del progetto ha riguardato l'analisi comparativa del profilo proteico sia della senescenza replicativa che della senescenza precoce indotta dallo stress ossidativo. Abbiamo evidenziato 20 spot proteici comuni alle due condizioni, differenzialmente rappresentati (3 up- e 17 down-regolati) in cui con la spettrometria di massa sono state identificate 25 componenti proteiche diverse. Per verificare se la down-regolazione di tali geni è basata su meccanismi di regolazione che agiscono a livello trascrizionale, i livelli degli mRNA delle 25 proteine sono stati analizzati nei due modelli di senescenza. Tra questi, 10 geni che presentavano almeno 2 volte di diminuzione di mRNAs nelle 2 condizioni, sono stati ulteriormente analizzati. Per corredare poi di significato funzionale la down-regolazione di queste proteine, abbiamo silenziato individualmente l'espressione di questi

10 geni con siRNA specifici nelle cellule IMR90 giovani. I risultati dimostrano che il silenziamento dei geni LEPRE1, LIMA1/EPLIN, MAGOHA e MAGOHB, induce un fenotipo senescente con presenza di marcatori specifici e mediato, nel caso di MAGOHA e MAGOHB, dall'attivazione del pathway di p53.

Abbiamo successivamente analizzato sia ai livelli proteici che di mRNA in: i) cellule IMR90 senescenti dopo danno al DNA; ii) in cellule WI38 senescenti per accorciamento dei telomeri, o stress ossidativo; iii) fibroblasti provenienti da donatori di età diversa compresa tra 21 e 94 anni. I risultati hanno dimostrato che nelle cellule senescenti, sia *in vitro* che *in vivo*, i livelli delle proteine e quelli dei rispettivi mRNA sono diminuiti.

Infine, poiché è noto che modifiche selettive degli istoni, in particolare la metilazione delle lisine dell'istone H3, giocano un ruolo cruciale nei meccanismi di regolazione dell'espressione genica a livello epigenetico, abbiamo verificato lo stato di metilazione dell'istone H3 dei promotori dei geni LEPRE1, LIMA1/EPLIN, MAGOHA e MAGOHB in condizioni di senescenza. A tale scopo abbiamo effettuato esperimenti di immunoprecipitazione della cromatina utilizzando anticorpi specifici per il marcatore repressivo H3K27me3 oppure per il marcatore attivatorio H3K4me3. I risultati dimostrano che l'espressione ridotta di tali geni nella senescenza è associata ad incremento della quantità di marcatore repressivo H3K27me3 ed in quasi tutti i casi a diminuzione del marcatore attivatorio H3K4me3.

In conclusione i dati ottenuti con l'approccio di proteomica differenziale hanno consentito di identificare nuovi geni (hnRNPA3 e RAD23B LEPRE1, LIMA1/EPLIN, MAGOHA, MAGOHB) che hanno un ruolo causativo nella comparsa del fenotipo senescente.

Tali risultati se da un lato contribuiscono all'approfondimento dei meccanismi molecolari della senescenza, dall'altro pongono le basi per considerare tali geni possibili marcatori dell'invecchiamento e delle patologie età-correlate, nonché candidati per sviluppare strategie terapeutiche per la manipolazione *in vivo* della senescenza cellulare.

Summary

Normal cells do not replicate indefinitely, rather after a certain number of divisions, they enter into a state of permanent arrest of proliferation defined cellular senescence.

Cellular senescence is accompanied by a reprogramming of gene expression profile, resulting in changes of the regulatory mechanisms that act at both transcriptional and post-transcriptional as well as at epigenetic level.

MicroRNAs (miRs) are small non-coding RNAs that play a fundamental role in the negative regulation of gene expression at post-transcriptional level. They recognize sequences in the 3'UTR and block the translation or determine the degradation of messenger RNAs.

In the laboratory had previously been identified 24 miRs (SAmiRs) up- or down-regulated in cellular senescence of primary fibroblasts IMR90. Functional studies on SAmiRs up-regulated demonstrated that 5 of them are able to induce premature senescence phenotype when over-expressed in young cells, in particular, the miR-494 elicited the most robust senescent phenotype.

Our studies have pursued two main objectives:

- i) to study the regulatory pathways in which is involved the miR-494 through the identification of its molecular targets;
- ii) to identify novel common mediators/effectors of cellular senescence induced by telomere shortening or caused by oxidative stress.

For both aims, we choose a *high-throughput* proteomic approach using the technology of 2D-DIGE (Two Dimensional-Difference Gel Electrophoresis) coupled to Mass Spectrometry (LC-MS / MS).

In the first objective, to identify possible targets of miR-494, we monitored with 2D-DIGE changes at the protein level consequent to its overexpression in cells IMR90 young, considering the inverse relationship between levels of miRs and protein levels of their targets. The 2D-DIGE analysis allowed us to consider about 1500 protein spots present in both of the two conditions. Among these, 102 protein spots (38 up- and 64 down-regulated) were differentially represented

in the cells transfected with miR-494, compared with control cells transfected with miR-scrable. Mass Spectrometry analysis identified 172 different protein species, of which 121 present in the spots down-regulated. In silico analysis, allowed the identification among these of 26 putative targets of miR-494, 9 of which have been selected by us for functional analysis. By using luciferase assays, we showed that four of them (hnRNPA3, PDIA3, RAD23B, SYNCRIP / hnRNPQ) contain functional binding sites for miR-494. We also showed that the expression of hnRNPA3, PDIA3, RAD23B, SYNCRIP decreased or increased in conditions of over-expression or inhibition of miR-494, respectively. The reduced expression of these proteins has also been found in other models of cellular senescence. We also showed that silencing hnRNPA3 or RAD23B in young IMR90 cells induces a senescent phenotype similar to that induced by the over-expression of miR-494, and mediated by the activation of the p53 pathway. Finally, other results have shown that the senescent phenotype induced by miR-494 is prevented if in the cells was introduced hnRNPA3 or RAD23B genes.

The other aspect of the project involved the comparative analysis of the protein profile occurring both in replicative senescence and premature senescence induced by oxidative stress. We showed that 20 protein spots common to both conditions are differentially represented (3 up- and 17 down-regulated) and in these the Mass Spectrometry identified 25 different protein components. To check whether the down-regulation of these genes is based on regulatory mechanisms that act at the transcriptional level, the levels of mRNAs of 25 proteins were analyzed in the above reported models of senescence. Among them, 10 genes that had at least 2 times decrease of mRNAs in both conditions, were further analyzed. Then, to study the functional significance of the down-regulation of these proteins, we individually silenced the expression of these 10 genes using specific siRNA in young IMR90 cells. The results show that silencing of LEPRE1, LIMA1/EPLIN, MAGOHA and MAGOHB genes, induces a senescent phenotype with the presence of specific markers and mediated, in the case of MAGOHA and MAGOHB, by the activation

of the p53 pathway.

We then looked at both protein and mRNA levels in: i) IMR90 senescent cells after DNA damage; ii) WI38 senescent cells caused either by telomere shortening or oxidative stress; iii) fibroblasts from donors of different ages between 21 and 94 years. The results showed that in senescent cells, both *in vitro* and *in vivo*, the levels of the proteins and those of the respective mRNAs are decreased.

Finally, since it is known that selective histone modifications, in particular the methylation of histone H3 lysine, play a crucial role in the mechanisms of gene expression regulation at epigenetic level, we verified the methylation status of histone H3 in the promoter genes of LEPRE1, LIMA1/EPLIN, MAGOHA and MAGOHB during senescence. For this purpose, we performed chromatin immunoprecipitation experiments using antibodies specific for the repressive H3K27me3 marker or for the active H3K4me3 marker. The results demonstrate that the reduced expression of these genes in senescence is associated with increase in the amount of repressive H3K27me3 and in almost all cases to decrease of active H3K4me3.

In conclusion, the data obtained with the approach of differential proteomics have identified novel genes (hnRNPA3 and RAD23B LEPRE1, LIMA1/EPLIN, MAGOHA, and MAGOHB) that have a causative role in the appearance of the senescent phenotype.

These results on one hand contribute to gain a deeper knowledge of the molecular mechanisms involved in senescence and on the other creates the basis for considering these genes as possible markers of aging and age-related diseases, as well as candidates for developing therapeutic strategies for the manipulation of *in vivo* cellular senescence.

Index

Pag.

1. Introduction

1.1 Cellular senescence: causes and markers	1
1.2 Cellular senescence: regulation of gene expression	4
1.3 Cellular senescence: molecular pathways	7
1.4 Cellular senescence: biological impact	11
1.5 Scientific hypothesis and aim of the work	13

2. Materials and Methods

2.1 Cell cultures and reagents	14
2.2 2D-DIGE coupled to Mass Spectrometry analysis	15
2.3 Bioinformatic analysis	17
2.4 Luciferase constructs and reporter assay	17
2.5 Western blotting	19
2.6 Reverse transcriptional and real-time qPCR	19
2.7 Senescence-associated β -galactosidase assay	20
2.8 Comet assay	21
2.9 Chromatin Immunoprecipitation (ChiP)-qPCR assays	21
2.10 Statistical analysis	23

3. Results

3.1 Proteomic analysis by Two Dimensional-Difference Gel Electrophoresis (2D-DIGE) coupled to Mass Spectrometry (MS) and bioinformatic prediction of putative miRNA-494 targets	24
3.2 hnRNPA3, PDIA3, RAD23B and SYNCRIP -3'UTRs are real direct targets of miR-494	30
3.3 hnRNPA3, PDIA3, RAD23B and SYNCRIP are down-regulated in different models of senescence	32
3.4 Functional effects of down-regulation of miR-494 targets in young IMR90 cells	34
3.5 Role of the miR-494 targets in the senescence program	38

3.6 Comparative proteomic analysis of IMR90 senescence induced either by telomere shortening or by oxidative stress	41
3.7 RNA interference-mediated knockdown of LEPRE1, LIMA1, MAGOHA and MAGOHB induces a senescent phenotype in IMR90 cells	45
3.8 Expression analysis of LEPRE1, LIMA1, MAGOHA and MAGOHB protein in other senescence models <i>in vitro</i> and <i>in vivo</i>	47
3.9 H3K4me3 and H3K27me3 changes of the LEPRE1, LIMA1, MAGOHA, and MAGOHB promoters during senescence	49
4. Discussion	51
5. References	55

List of Tables and Figures

	Pag.
Table MM1. Oligonucleotides sequences for Luciferase-3'UTRs constructs	18
Table MM2. Oligonucleotides sequences for hnRNPA3-FLAG and RAD23B-FLAG constructs	18
Table MM3. Oligonucleotides sequences for RT-qPCR assay	20
Table MM4. Oligonucleotides sequences for Chip-qPCR assay	23
Table 1. List of the 26 putative miR-494 targets predicted by <i>in silico</i> computational analysis	28-9
Table 2. List of the common proteins identified as differentially represented in replicative (PDL58) and DEM-senescent IMR90 cells by 2D-DIGE and nLC-ESI-LIT-MS/MS analyses	44
Figure 1. Causes and hallmarks of cellular senescence	3
Figure 2. Pathways involved in cellular senescence	10
Figure 3. Proteomic strategy based on 2D-DIGE/MS analysis coupled to bioinformatic prediction of miRNA-494 targets	26
Figure 4. hnRNPA3, PDIA3, RAD23B and SYNCRIP are direct targets of miR-494	31
Figure 5. hnRNPA3, PDIA3, RAD23B and SYNCRIP are down-regulated in different models of senescence	33
Figure 6. Functional effects of hnRNPA3 and RAD23B down regulation in young IMR90 cells	36
Figure 7. Ectopic expression of hnRNPA3 or RAD23B in young IMR90 cells hampers the senescence process induced by miR-494	39
Figure 8. Comparative 2D-DIGE and transcriptional analysis of	

genes identified in spots common to both conditions of senescence	43
Figure 9. Functional effects of down-regulation of LEPRE1, LIMA1, MAGOHA and MAGOHB in young IMR90 cells	46
Figure 10. Protein levels of LEPRE1, LIMA1, MAGOHA and MAGOHB in other senescence models	48
Figure 11. Analysis of H3K4me3 and H3K27me3 states on LEPRE1, LIMA1, MAGOHA and MAGOHB promoters in IMR90 senescent cells	50

1. Introduction

1.1 Cellular senescence: causes and markers

Cellular senescence was described for the first time in 1961 by Hayflick and Moorhead as an inevitable and irreversible cell-cycle arrest after a series of passages in culture of normal fibroblasts (1). In fact, the life span of primary normal cells is determined by a limited number of divisions, called the *Hayflick limit*, after which cells arrest, usually in the G1 phase, and no longer respond to growth factors. This phenomenon also known as “replicative senescence”, is causally linked to telomere attrition. In normal human fibroblasts telomeres shorten progressively at each cell division and when they reach a critically short length, the cell perceives this as a persistent DNA damage, a primary cause of the senescence onset.

Initially, cellular senescence was considered an artefact of culture and its contribution to organismal aging was only hypothesized (1). Recent studies demonstrate that replicative senescence also occurs *in vivo* and in other cell types including keratinocytes, endothelial cells and lymphocytes. Furthermore, different stressors have also been demonstrated to induce prematurely a similar phenotype of senescence, called premature senescence. Thus, more generally, senescence can be considered as a state of stable cell cycle arrest in response to diverse types of stress (2). These stressors can be intrinsic or extrinsic and include activated oncogenes such as mutated forms of RAS or BRAF, loss of tumor suppressors genes, i.e. PTEN, NF1, increased oxidative stress, ionizing/ultraviolet radiations (2-6). Most of these stimuli can directly or indirectly induce DNA damages that in turn trigger a DNA damage response (DDR) (**Figure 1**) (7). When DDR becomes persistent, the cells activate prematurely the senescence program. Persistent DDR signaling, initiated both at telomeric and non-telomeric sites, drives also senescence *in vivo* (8), whose importance is now recognized in aging and age-related pathologies as well as in tumor suppressor mechanism (3,9).

Senescent cells show a distinct morphology with an enlarged and flattened shape, prominent nucleoli and cytoplasmic granules, and also produce specific markers, that include overproduction of Reactive

Oxygen Species (ROS), formation of heterochromatic foci (SAHF) derived from reorganization of chromatin, presence of DNA damage foci (SDF) and promyelocytic leukemia protein nuclear bodies (PML NBs), increased lysosomal β -galactosidase activity at pH 6 (Senescence-Associated β -gal, SA- β -gal), some of which are used to detect senescent cells also *in vivo* (10).

Furthermore, senescent cells acquire a specific secretory phenotype called SASP (Senescence-Associated Secretory Phenotype) or SMS (Senescence-Messaging Secretome) enriched for pro-inflammatory cytokines, chemokines, growth factors, and metalloproteases that could affect positively or negatively the tissue homeostasis. Among these, certain cytokines and chemokines, in particular interleukin-6 (IL-6) and interleukin 8 (IL8) as well as its receptors appear to reinforce the proliferative arrest, promote immune clearance of damaged cells, communicate to the surrounding cells the state of senescence, thus influencing positively the behavior of adjacent cells. Paradoxically, persistent activity SASP factors can have negative effects by causing chronic inflammation, disturbing tissue architecture and stimulating phenotypes associated with both cancer initiation and growth (11).

Another characteristic of senescent cells is the altered reactivity to apoptotic stimuli. Indeed, many senescent cells are resistant to apoptotic signals, related to the increase of the anti-apoptotic protein bcl2 and reduction of caspase-3. This resistance may explain why senescent cells accumulate in tissues with age, although it has recently been shown that there is an important mechanism for the removal of senescent cells (clearance) by the immune system (12).

All the above characteristics are tightly associated with a global change in the gene expression profiles (8,13). In fact, senescent cells up-regulate numerous genes involved in cell cycle arrest as well as in the production of SASPs and down-regulate genes controlling cell cycle progression. Modifications of gene expression are governed at transcriptional, post-transcriptional and epigenetic levels.

Introduction

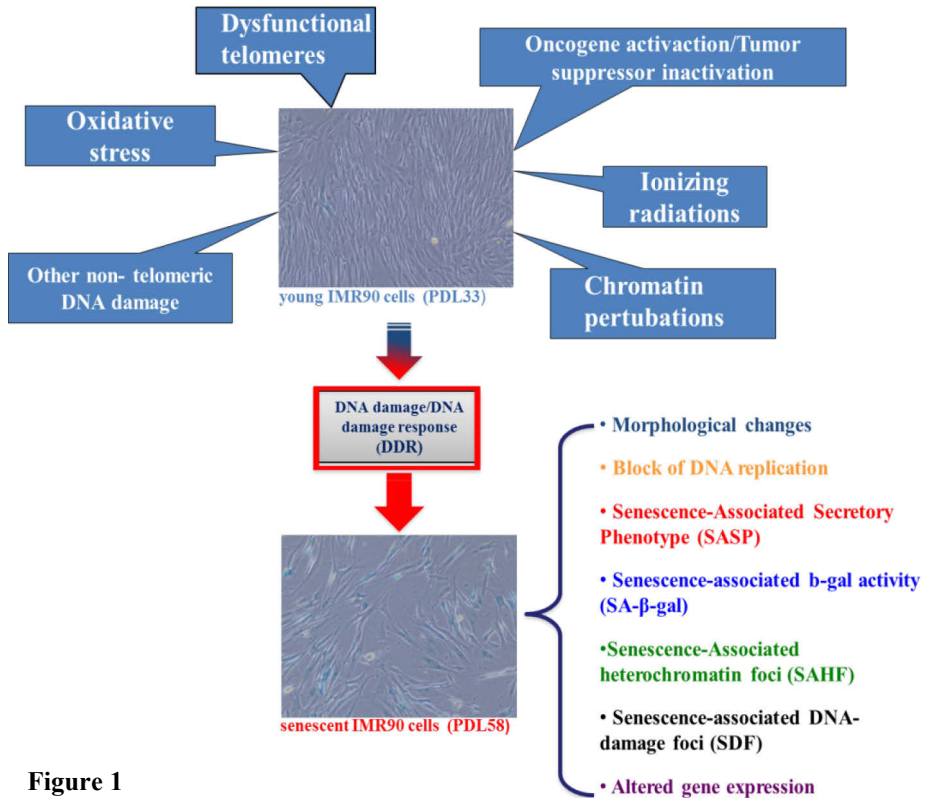


Figure 1

Figure 1: Causes and hallmarks of cellular senescence.

Cellular senescence is a permanent cell cycle arrest triggered by different type of stresses, that result in DNA damage, which in turn triggers a DNA damage response (DDR). When DDR becomes persistent, cells activate the senescence program.

The senescent cells acquire specific hallmarks of senescence such as: morphological changes, absence of duplications, secretion of various molecules (SASP), positive staining for Senescence-Associated beta-Galactosidase activity (SA-β-Gal), appearance of Senescence-Associated heterochromatin foci (SAHF) and Senescence-Associated DNA-damage foci (SDF). All these marks are supported by a global change of gene expression.

1.2 Cellular senescence: regulation of gene expression

Modification of gene expression is a major determinant for the induction of the senescence program, in which are involved specific alterations of transcriptional and post-transcriptional events as well as epigenetic regulatory mechanisms (14-18)

This transcriptional program involves modification of cell cycle-related genes with down-regulation of genes promoting cell cycle along with up-regulation of p21 and p16^{INK4a} genes governing cell arrest and many others genes with other functions including some with enzymatic activity (i.e. β -galactosidase, matrix-remodeling proteases) as well as inflammatory chemokines, cytokines and growth factors (19).

A key regulatory factor involved in transcriptional regulation of genes implicated in cell cycle arrest such as p21, GADD45A, RPRM (20) is p53 that will be discussed later (in the section 1.3).

The induction of cell cycle arrest is also dependent on the Retinoblastoma (Rb) protein family that contains the three members Rb, p107 and p130. Among these, Chicas et al. (21) demonstrated that Rb is the main factor for determining the permanent cell cycle arrest, unique to senescence, by inhibition of E2F-dependent transcription of a subset genes specifically involved in DNA replication. A recent study of Vernier et al. (22) reported that in senescent cells Rb/E2F complexes localize in PML nuclear bodies along with heterochromatin protein 1 (HP1) and Rb phosphatase PP1 α (protein phosphatase 1 α). Since HP1 has a causal role in chromatin architecture changes, and PP1 α contributes to the hypophosphorylated-Rb status, the proposed model is that PML NBs could be the site of “nucleation” or initiation of the heterochromatinization of E2F target genes.

Given that senescent cells secrete numerous soluble factors known as SASP, a specific transcriptional program inducing expression of these genes is activated by the transcription factors NF- κ B and C/EBP β (11). NF- κ B contributes to the senescence by reinforcing growth arrest and activating IL6 and IL8 gene transcription. These genes are also regulated by C/EBP β that is mainly required for cellular senescence induced by oncogenic stress. Moreover, the activity of NF- κ B and

C/EBP β is regulated by the IL1 signaling (also known as inflammasomes) (23,11), thus creating a positive feedback loop that contributes to the establishment of the senescence program.

Another mechanism of gene regulation that acts at post-transcriptional level involves microRNAs (miRNAs) (24). miRNAs are a class of short (around 22 nucleotides) non-coding RNA molecules that behave as negative modulators of gene expression. miRNAs recognize complementary sequences that are generally localized in the regions of the 3' untranslated (3'UTRs) of target mRNAs and function with a sequence-specific silencing mechanism (25).

Most of the genes for miRNAs are transcribed from RNA polymerase II (Pol II) as long precursors transcripts that form a hairpin stem loop structure necessary for the processing into pre-miRNAs by a multiproteic complex, called "Microprocessor" consisting of Drosha (RNase III endonuclease) and DiGeorge syndrome critical region 8 (DGCR8) (26). pre-miRNAs are 60- to 70-nucleotide long and are then transported to the cytoplasm by Exportin 5 where they are further processed to duplex RNAs of about 22 nucleotides (miRNA:miRNA*) by Dicer. The mature miRNA originated from Dicer activity is guided to the target mRNAs by base-pairing interactions, after its incorporation into the RNA-induced silencing complex (RISC). The mechanisms proposed for miRNA-mediated activity are three: i) miRISC could mediate the repression of translation by competition between Ago2 and eIF4E for cap binding, ii) miRISC could stimulate the deadenylation of the mRNA tail that causes degradation of the mRNAs, iii) the miRISC could also block association of ribosomal subunits (26).

Given that each single miRNA could targets many transcripts (up to hundreds), miRNAs might influence a large variety of cellular processes (27). Recent findings, also obtained in our laboratory (28), show that miRNAs are regulated during cellular senescence and, in turn, are able to trigger senescence (29–32) by affecting specific genes involved in DDR, telomere protection/attrition, homeostatic processes, as well as genes involved in gene expression regulation, thereby affecting transcriptional, post-transcriptional and epigenetic changes (33). We have reported that 5 miRNAs, (miR-210, miR-376a*, miR-

486-5p, miR-494, miR-542-5p), which are up-regulated during the senescence process of primary human diploid IMR90 fibroblasts, activated a premature senescence program when overexpressed in young cells. Among them, miR-494 elicited the most robust effects by inducing features such as reduced cell proliferation, induction of SA- β -gal, SAHFs, DNA damage, SDFs, and reactive oxygen species (ROS) accumulation (28). Another miR that resulted up-regulated in these studies is miR-210. Regarding miR-210, a recent paper demonstrated that its role in senescence is also linked to the direct repression of Polycomb group protein (PcG) members that are involved in the inactivation of the p16^{INK4a} encoding gene (34).

The above results exemplify another important mechanism of gene expression regulation: the epigenetic modifications that are also fundamental for the induction/establishment of cellular senescence (33). Among these, selective histone modifications play a critical role in the patterns of gene expression associated to senescence. In fact, the formation of senescence-associated heterochromatin foci (SAHF) responsible for E2F target genes silencing (35) or the activation of the INK4A-ARF locus that encodes p16^{INK4a} (36, 37) involves modifications of the methylation status of the lysines within the H3 histone. SAHFs, indeed, are characterized by H3 bearing trimethylated Lys9 (H3K9me3) that acts as a repressive mark, whereas the INK4A-ARF locus displays a decreasing level of trimethylated Lys27 (H3K27me3) behaving as a repressive mark. Of note, the miR-210 post-transcriptional regulation of PcG proteins establishes a cross-talk in senescence between microRNAs and epigenetic regulators of transcription.

Very recently, genome-wide studies have associated lamin B1-dependent chromatin reorganization upon senescence not only to SAHF formation but also to gene expression regulation. In fact, local increase of H3K27me3 facilitated repression of a subset of genes involved in cell proliferation (38), whereas depletion of H3K4me3 and H3K27me3 paralleled with down- and up-regulation of proliferating and SASP genes, respectively (39). An increase of repressive marks and a decrease of active marks were also observed during oncogene-induced senescence (40).

1.3 Cellular senescence: molecular pathways

The molecular determinants that establish the enter in senescence are not fully understand. However, telomere shortening-related replicative senescence, occurring *in vivo* and *in vitro*, and premature senescence are governed by a persistent DNA damage response (DDR) (41,42). In general, this event engages various cellular signalling cascades that ultimately activate p53 or p16^{INK4a}, or both (43,44) (**Figure 2**). Very interestingly the levels of both proteins, especially those of p16^{INK4a}, correlate with chronological ages in humans and in mice. (33). The relative contribution of these pathways is dependent on cell type, and the types of insults. (44)

p53, also known as tumor protein 53 (TP53), is a transcription factor that regulates a variety of cellular responses, including cell cycle arrest and DNA repair as well as apoptosis, metabolism and senescence (45). It plays the role of tumor suppressor and is recognized as "the guardian of the genome" referring to his function in maintaining the genome stability by preventing/repairing mutations that could initiate tumorigenic events.

In normal cells, p53 is usually inactive, bound to MDM2 protein that promotes its degradations working like an ubiquitin ligase. After initial events of DNA damage, cells activate a p53-dependent transient cell cycle arrest to induce repair of DNA. When the DNA damage is irreparable, in particular involves DNA double strand breaks (DSBs), the arrested state becomes permanent (senescence). The DSBs are detected by the MRN (MRE11, RAD50, NBS1) complex that promotes auto-phosphorylation and activation of ATR (Ataxia Telangiectasia and Rad3 related) or ATM (Ataxia Telangiectasia Mutated) leading to the subsequent phosphorylation of specific ATR/ATM substrates. One of these is the histone variant H2AX that in phosphorylated state (γ -H2AX) accumulates to sites of DNA damage and induces changes in local chromatin structure. These γ -H2AX foci presumably attract specific repair factors, including ATM its self. In this platform the protein 53BP1 is responsible for the recruitment of p53 that undergoes stabilization and ATM-dependent phosphorylation at serine 15. In addition, p53 can also be

phosphorylated by the checkpoint kinase CHK2 that along with CHK1 is activated by different types of DNA damage (46).

Once activate, p53 induces transcription of many genes (20,47) including p21 and PML (promyelocytic leukemia) which are also recognized as markers of senescence. The p21 gene encodes a potent cyclin-dependent kinase (CDK) inhibitor, called p21 (also known as WAF1) that generally arrests cell-growth in G1 phase. Indeed p21 inhibits the activity of cyclin-CDK2 or CDK4 complexes, with a subsequent block of E2F- and PCNA-dependent cell cycle progression. PML is the major structural component of PML nuclear bodies that are increased during senescence (48). PML and p53 activity are interlinked because p53 activates the transcription of PML that in turn interacts with both p53 and MDM2. Thus, beside MDM2, the p53 activity is under the control of the PML protein, which operates a positive feedback on the p53-dependent pathways of senescence (48). Furthermore, PML by recruiting the complex pRb/E2F, also contributes to cellular senescence induced by p16^{INK4a}/Rb-dependent pathways (22).

Of note, cellular senescence could be also activated by p53-independent mechanisms as demonstrated for the inactivation of VHL tumor suppressor (49) or inactivation of the oncogenic protein Sk2p in the context of both PTEN or ARF loss (50) as well as for programmed senescence occurring during development (51, 52). Additionally, it has been also demonstrated that senescence can be induced through a DDR-independent manner. For example BRAF (V600E) induces an unusual senescence through a metabolic effector pathway. BRAF (V600E) activates PDH (pyruvate dehydrogenase) by inducing PDP2 and inhibiting PDK1 expression, promoting a shift from glycolysis to oxidative phosphorylation that creates senescence-inducing redox stress associated to the release of SASP factors (53).

p16^{INK4a}/pRb pathway is mainly activated in premature senescence and is regarded as a principal marker of senescent cells *in vivo*. p16^{INK4a} is encoded by the INK4/ARF locus that also encoded for ARF, an upstream positive regulator of p53 (54). p16^{INK4a} by inhibiting the activity of CDK4 and CDK6, prevents the phosphorylation of Rb, thus blocking the release of E2F required for

Introduction

transcription of genes promoting proliferation (54). On the contrary, the hyperphosphorylation of Rb allows the progression of the cell cycle. Thus, both pathways of p16^{INK4a} and p53/p21 converge into retinoblastoma protein and by repressing its phosphorylation prevent the E2F activity, thereby leading to cell cycle arrest.

Several studies demonstrated that p16^{INK4a} has also other functions. For example, up-regulation of p16^{INK4a} in human mammary epithelial cells mediates silencing of the hTERT promoter through histone 3 lysine 27 trimethylation (55).

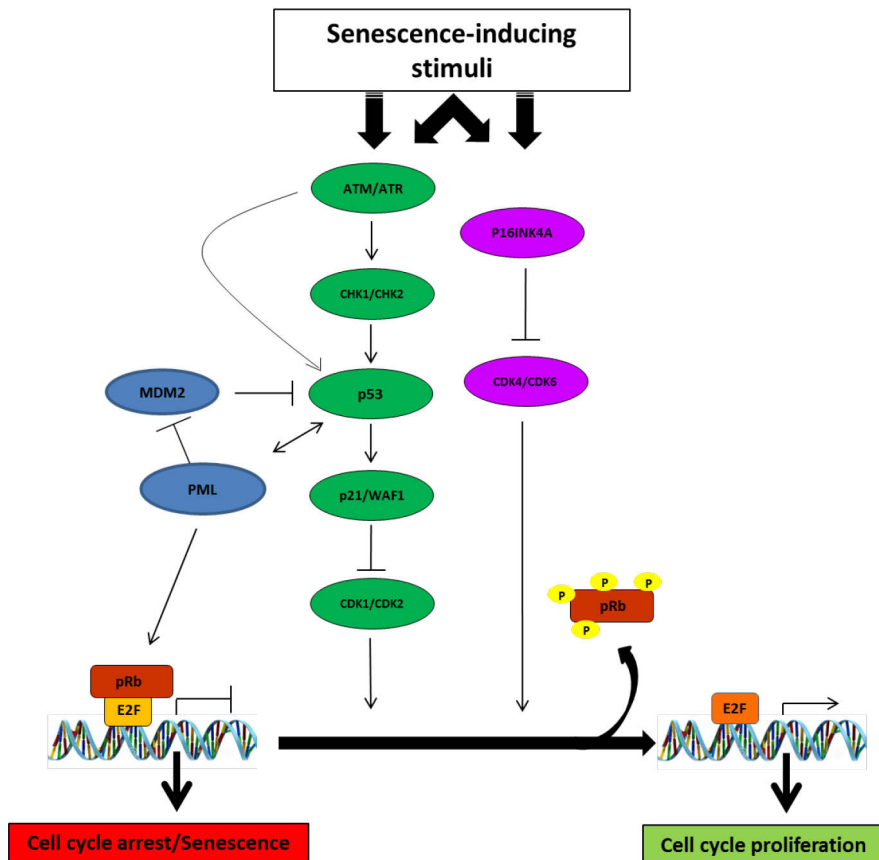


Figure 2

Figure 2: Pathways involved in cellular senescence.

The senescence-inducing stresses are able to engage various cellular signalling cascades that, depending on the type of stress, involve p53/p21 or p16^{INK4a}, or both pathways. They, through activation of cell cycle inhibitors, lead to phosphorylation of tumor suppressor pRb. When pRb becomes hyper-phosphorylated, its binding to E2F is inhibited and this allows the transcription of several E2F-target genes, most of which are involved in the G1/S transition phase.

1.4 Cellular senescence: biological impact

Numerous studies in the last 10 years have demonstrated that cellular senescence occurs *in vivo* and has both physiological and pathological consequences on the functionality of the organism (12,56).

It is now largely accepted that cellular senescence represents a failsafe program activated in response to potential oncogenic events, thus reducing the risk of neoplastic transformation. In fact, replicative senescence imposes a self-limiting proliferative capacity when genomic damages, such as telomere shortening, could initiate/fuel tumorigenesis and premature senescence arrests the propagation of cells with non-telomeric irreparable damage DNA or with aberrant activation of oncogenes caused by mutations (i.e. RAS, RAF) referred as oncogene-induced senescence (OIS), as well as with loss of tumor suppressors (i.e. PTEN, VHL). According to this, in human nevi that frequently harbor mutations in BRAF, cells possess positive markers for senescence such as overexpression of p16^{INK4a} (57) and in PTEN-deficient tumorigenesis a p53-dependent senescence has been also described (58).

In addition to its function as tumor suppressor, another positive role of cellular senescence *in vivo* has been shown in tissue damages of different tissues. In particular, in a mouse model of liver fibrosis has been demonstrated that the senescence of fibrogenic myofibroblasts by producing SASPs containing extracellular matrix-degrading enzymes as well as cytokines, and by recruiting cells for immune surveillance, could limit fibrosis during tissue repair (12). Similarly, in the skin wound healing, senescence could represent a mechanism for controlling fibrinogenesis (56).

Furthermore, very recently has been demonstrated that cellular senescence also occurs during the embryonic development. In this context, it plays an important physiological role associated with instructing tissue growth and organ patterning (51, 52). The embryonic senescent cells do not activate DDR and p53 or p16^{INK4}, but display some features i.e. production of SASP and induction of p21 dependent on SMAD and FOXO transcription factors (52).

Although these beneficial roles, cellular senescence is now considered

a crucial contributor to organismal aging and age-related diseases. In this context, *in vivo* accumulation of senescent cells with age not only impacts negatively on the functionality of tissues but also limits tissue renewal as a consequence of adult stem cells senescence.

Although its specific relevance *in vivo* needs further investigations, the activities of SASP seem to be key contributors for both physiological and pathological consequences of senescence in the organism. Transient SASP components such as IL6 and IL8 can indeed reinforce the senescence in an autocrine fashion as well as recruit cells of immune system to eliminate senescent cells, thus contributing positively on the senescence-tumor suppressor activity in the organism. On the contrary, a persistent SASP activity, in particular due to IL1, can act in a paracrine fashion by promoting both chronic inflammation, that has a predominant role in various age-related pathologies, and senescence in neighbouring cells that could disturb architecture and functionality of tissues. These conditions can also stimulate events that contribute to a pro-tumorigenic state in surrounding cells (11,59).

It is now generally accepted that senescent cells accumulate during the life of the organism and contribute to aging and age-related diseases. Recently, the van Deursen group has demonstrated that inducible elimination of p16^{INK4a}-positive senescent cells in BubR1 progeroid mouse model delayed the onset of age-related phenotypes in several tissues such as eye, adipose and skeletal. They showed that elimination of p16^{INK4a}-positive cells also attenuated the progression of already established age-related disorders, thus suggesting that cellular senescence may have a causal role in age-related tissue impairment (19).

1.5 Scientific hypothesis and aim of the work

Cellular senescence is tightly associated with a global change in the gene expression profile. Modification of gene expression involves specific alterations of transcriptional and post-transcriptional events as well as epigenetic regulatory mechanism.

The major contributors of post-transcriptional regulation of gene expression are microRNAs (miRNAs). Recent findings, obtained also in our laboratory, show that miRNAs are regulated during cellular senescence and, in turn, are able to trigger senescent phenotype. We reported that ectopic expression of 5 miRs which are up-regulated during senescence of human diploid IMR90 fibroblasts, promoted a premature senescent phenotype. Among them, miR-494 elicited the most robust effects, including reduced of cell proliferation, induction of SA- β -gal activity, appearance of SAHFs, DNA damage, SDFs and accumulation of reactive oxygen species (ROS).

Specific modifications of selective histones play a critical role in epigenetic-associated regulatory mechanisms. Of note, the methylation status of the lysines within the H3 histone particularly contributes to the stability of the senescent phenotype, as exemplified by the formation of senescence-associated heterocromatin foci (SAHF) that are responsible for E2F target genes silencing or INK4A-ARF locus activation, both essential for the senescence onset.

In this study we used a proteomic approach, particularly 2D-DIGE coupled to Mass Spectrometry analysis, to follow two main objectives:

- To identify novel direct targets of miR-494 in human diploid IMR90 fibroblasts that could play a crucial role in the induction of the senescence program and to investigate the functional effects after their manipulations in young and senescent cells.
- To identify novel genes acting as common mediators of the senescence induced either by telomere shortening or by oxidative stress in IMR90 cells and to study the effects of their manipulation, the epigenetic regulation of their expression as well as the relevance *in vivo* of these findings.

2. Materials and Methods

2.1 Cellular cultures and reagents

Normal human primary fibroblasts IMR90 were obtained from Coriell Institutes for Medical Research (CCR; New Jersey, USA). Cells were cultured in Dulbecco's modified Eagle's medium (DMEM) (Invitrogen, Groningen, The Netherlands) supplemented with 10% v/v fetal bovine serum and 1% penicillin/streptomycin (Invitrogen). WI38 at passage 11 (p11) or 15 (p15) were kindly provided by Fabrizio d'Adda di Fagagna (Istituto di Oncologia Molecolare, Fondazione Italiana per la Ricerca sul Cancro, Milan, Italy) and cultured in modified Eagle's medium supplemented with 10% FBS, 10 mM non-essential amino acids, and 1 mM sodium pyruvate (Invitrogen) until passage 23 (p23). The population doubling level (PDL) was calculated by using the formula $PDL = \log(n_h/n_i)/\log 2$, where n_i is the initial number of cells and n_h is the final number of cells at each passage. To induce premature senescence, IMR90 at PDL34 or WI38 cells at PDL30 were treated with 100 μ M diethylmaleate (DEM) (Sigma-Aldrich) for ten days (28).

Primary fibroblast cell lines from healthy donors of different ages were obtained from CCR. Cells lines from young donors were AG09309 (21 years, skin, PDL12), AG10803 (22 years, skin, PDL11.7) and AG09319 (24 years, gingival, PDL9) and were grown in Essential Medium with Earl's salts/non-essential amino acids (both from Lonza, Switzerland) supplemented with 10% or 15% v/v fetal bovine serum (according to CCR's instructions) and 1% penicillin/streptomycin (Invitrogen), at 37 °C, in a 5% CO₂-humidified atmosphere. Cells lines from old donors were AG05247 (87 years, skin, PDL15), AG10884 (87 years, skin, PDL7), AG04064 (92 years, skin, PDL16.41), AG09602 (92 years, skin, PDL5.48), AG08433 (94 years, skin, PDL15.52) (60, 61). These were grown in Eagle's Minimum Essential Medium (MEM) containing Hank's BSS, 26 mM Hepes (Lonza) and supplemented with 15% v/v fetal bovine serum and 1% penicillin/streptomycin (Invitrogen), at 37 °C, in a 5% CO₂-humidified atmosphere.

Transfections of young IMR90 cells (PDL33) with synthetic premiRs

(100 nM; Invitrogen) and miRcury LNA microRNA inhibitors (100 nM; Exiqon, Vedbaek, Denmark) were performed by electroporation with a Microporator MP100 (Euro-Clone, Milan, Italy), as described previously (28). Transfections of small interfering RNAs (siRNAs; 25 or 50 nM; Qiagen, Hilden, Germany) were performed using Lipofectamine RNAiMAX transfection reagent (Invitrogen) with the reverse protocol, following manufacturer's suggestions with the reverse protocol, according to manufacturer's instructions. All the plasmids bearing 3'-UTR fragments were transfected in IMR90 cells with Lipofectamine 2000 (Invitrogen) in 48-well plates (20,000 cells/well), according to manufacturer's instructions.

2.2 2D-DIGE coupled to Mass Spectrometry analysis

In our studies, we have analyzed the differential protein expression by 2D-DIGE in:

- IMR90 cells (PDL33) transfected with premiR-494 and compared to premiR-scramble (control).
- two conditions of senescence, IMR90 at PDL58 and IMR90-DEM, compared to young IMR90 cells.

For both experiments, total proteins, from three independent biological replicates of each condition, were extracted with UTC solution (7 M urea, 2 M thiourea, and 4% w/v 3-[(3-cholamidopropyl)dimethylammonium]-1-propane sulfonate). Lysates were precipitated in 8:1 v/v acetone/methanol for 16 h, at -20°C , and centrifugated at $16,000 \times g$ for 30 min, at 4°C . Protein pellets were dissolved in UTC solution and samples (30 μg in a final volume of 10 μL) were labeled with the appropriate CyDye (240 pmol of Cy2, Cy3, or Cy5) according to the DIGE minimal labeling protocol (GE Healthcare, Milan, Italy) by implementation of a dye-swapping strategy (62). An equal mixture of all three samples of each biological replicate was labeled with Cy2 as internal standard during gel electrophoresis to allow gel-to-gel matching and in-gel analyses of relative protein spot intensities. Three sample mixtures, made of appropriate Cy3- and Cy5-labeled pairs and a Cy2-labeled control, were supplemented with UTC solution containing 130 mM DTT, 2%

immobilized pH gradient (IPG) buffer (pH 3–10 NL), and 2.8% DeStreak reagent (GE Healthcare, Little Chalfont, UK), and used for passive hydration of immobilized pH gradient (IPG) strips (24 cm) to run the isoelectric focusing on IPGphor II apparatus (GE Healthcare). After the first dimension, the strips were equilibrated and transferred into 12% polyacrylamide gels to perform the second dimension. SDS-PAGE was performed on a DALT II electrophoresis unit (GE Healthcare) at 1 W/gel for 16 h. Gels were scanned on a Typhoon 9400 variable mode imager (GE Healthcare), with the indicated excitation/emission wavelengths for Cy2 (488/520 nm), Cy3 (532/580 nm), and Cy5 (633/670 nm). 2D-DIGE images were acquired in the Image Quant software (GE Healthcare) and analyzed by using the DeCyder 6.0 software (GE Healthcare). A DeCyder differential in-gel-analysis module was used for spot detection and pairwise comparison of each sample (Cy3 and Cy5) to the Cy2 mixed standard present in each gel. The DeCyder biological variation analysis module was then used to simultaneously match all of the protein-spot maps from the gels, and to calculate average abundance ratios and p values across the triplicate sets of samples (Student's t-test). Only protein spots with a value of $p < 0.05$ were investigated further.

For preparative protein separations, 600 μg of unlabeled total proteins from pooled IMR90 at PDL34, IMR90 at PDL58 and IMR90-DEM extracts were used for passive hydration of 24 cm strips for the first gel dimension (pH 3–10 NL IPG strips, GE Healthcare). The first and second-dimension runs were carried out as described above. After 2-DE, gels were fixed and stained with SyproRuby fluorescent stain (Invitrogen-Life Technologies Italia, Monza, Italy). Finally, spots were matched with those of master gel from the analytical step in the biological variation analysis module of DeCyder software to generate a pick list for spot picking by a robotic picker (Ettan spot picker, GE Healthcare).

Afterwards, the spots were excised from the relative preparative gel and were processed for protein identification by Mass Spectrometry analysis (63). This analysis was performed in collaboration with the laboratory of Prof. Andrea Scaloni (Laboratorio di Proteomica e Spettrometria di Massa, ISPAAM, Consiglio Nazionale delle

Ricerche, Napoli, Italia).

2.3 Bioinformatic analysis

For the identification of miR-494 putative targets, 5 different software algorithms were used, namely TargetScan 6.2 (<http://www.targetscan.org>), miRanda (<http://www.microna.org>), miRDB (<http://mirdb.org>), PITA (<http://genie.weizmann.ac.il>), and RNA hybrid (<http://bibiserv.techfak.uni-bielefeld.de/rnahybrid/welcome.html>). The intersection of ≥ 3 programs resulted in a list of 26 genes as potential targets for miR-494 (Table 1).

2.4 Constructs and reporter assay

The 3'-UTR fragments containing miR-494 binding sites of candidate genes were amplified by PCR using human IMR90 DNA with primer pairs containing *Xba*I and *Bam*HI sites (Table MM1). The PCR products were cloned into the pGL3-control vector, downstream from the Firefly luciferase 3'-UTR (Promega, Madison, WI, USA). The orientation of the inserted fragments was established by digestion and confirmed by sequencing. The pGL3 constructs with the reverse orientation were used as negative controls. The pGL3 constructs with mutated target sites for miR-494 were generated using specific primers (Table MM1) and the QuikChangeMutagenesis kit (Agilent Technologies, Santa Clara, CA, USA).

The pGL3 constructs (100 ng) were cotransfected with the *Renilla* luciferase reporter plasmid (20 ng) as an internal control using Lipofectamine 2000 (Invitrogen). Luciferase activity was measured at 48 h after transfection of IMR90 cells using a dual luciferase reporter assay (Promega) according to manufacturer's instructions and performed on a 20/20n Luminometer (Turner BioSystems, Sunnyvale, CA, USA). Relative luciferase activity was calculated by normalizing the firefly luminescence to the *Renilla* luminescence.

Plasmids driving the expression of FLAG-hnRNPA3 or FLAG-RAD23B were prepared by inserting into the *Eco*RI/*Bam*HI-digested

Materials and Methods

p3xFLAG-CMV 7-1 plasmid (Sigma-Aldrich) the coding regions of human hnRNP3 [Integrated Molecular Analysis of Genomes and Their Expression (IMAGE) Consortium ID: 8322522] or human RAD23B (IMAGE ID: 3906269) (Thermo Scientific Italia, Rodano, Italy) obtained with specific primers (Table MM2) by polymerase chain reaction (PCR). IMR90 cells at PDL33 were first transfected with expressing plasmids using Lipofectamine 2000 (Invitrogen) for 24 h and sequentially transfected with synthetic premiRs (100nM) by using Lipofectamine RNAiMAX transfection reagent.

Table MM1: Oligonucleotides sequences used for wild type (WT) and point mutation (MUT2) Luciferase-3'UTRs constructs ("seed" interacting sequences are in bold and mutated bases are underscored).

Gene name	Forward primer sequence	Reverse primer sequence
hnRNP3-WT	5'-ATCATCTAGAGGA ^{CC} GTAGGAA ^{TG} TTAGGCTACTA-3'	5'-ATCATCTAGGAATCACA ^{GA} ACAT ^{GTG} GAAAT-3'
PDIA3-WT	5'-ATCATCTAGAGGA ^{AT} CCCCAGG ^{AG} CTGAGCTTAC-3'	5'-ATCATCTAGAGAA ^{GG} TACTGG ^{CT} TTCCCA-3'
RAD23B-WT	5'-ATCATCTAGAGGA ^{AT} CCCTCC ^{CC} CAGCAGAAAGG-3'	5'-ATCATCTAGATACCA ^{AT} CTTCCTTTT ^{GG} AAAGCAATA-3'
SYNCRIP-WT	5'-ATCATCTAGAGGATCCAA ^{AT} CGACAA ^{TGT} ACAGGGAA-3'	5'-ATCATCTAGACCAATGA ^{AT} CACTAT ^{GTG} CAAAAT-3'
hnRNP3-MUT2	5'-CAGAAG ^{GT} CTGTAA ^{TG} GAATCAGAA ^{TCA} <u>AT</u> CATTGTGATATAA ^{TG} AAATG-3'	5'-CAATTCATATACTACA ^{AA} <u>AT</u> ^{GTG} A ^{CT} GAATCCATTACAGAAC ^{CT} CTGTG-3'
PDIA3-MUT2	5'-GCATCCAGCAGTTTCA ^{CC} AA ^{GT} <u>TA</u> ATCAGGAAT ^{TC} GTGACACT ^{GT} GTG-3'	5'-CAGCAG ^{GT} TCAGCAAT ^{TC} <u>TA</u> ^{TTG} A ^{CT} TTGGAATCGA ^{AA} ACTCGCGAT ^{GT} GC-3'
RAD23B-MUT2	5'-GC ^{GT} ATTCAGTCAAA ^{TT} AATGCAAA ^{TCA} <u>AT</u> CAAACTGG ^{TT} CTGATA ^{TT} GTG-3'	5'-CAAATCAGAA ^{AC} CCAG ^{TT} TGAT ^{GTG} ATTGCA ^{TT} AATTTGAA ^{CT} GAA ^T CA ^{GC} -3'
SINCRYP-MUT2	5'-GAATAGTGGTGC ^{CA} AATG ^{CC} TGTAT ^{CA} <u>AT</u> CACTAA ^{TG} TTTTTT ^{GT} TATC-3'	5'-GATACAAA ^{AA} CAATTA ^{AT} GTGAT ^{GTG} A ^T ACAGGCTAT ^{GG} CA ^{CC} ACTAT ^{TC} -3'

Table MM2: Oligonucleotides sequences for hnRNP3-FLAG and RAD23B-FLAG constructs

Gene name	Forward primer sequence	Reverse primer sequence
hnRNP3-FLAG	5'-CAACTGGAATTCGGAGGTA ^{AAAA} CCGCCGCC-3'	5'-ATAGCGGATCCTTAGAACCTCTGTACCATATC-3'
RAD23B-FLAG	5'-ATAGCGAATTCGAGGTCAC ^{CC} CTGAAGACC-3'	5'-ATAGCGGATCCTCAATCTTCATCAAAGTTCTGCT-3'

2.5 Western blotting

Cells were lysed by resuspension in a buffer containing 0.02 M HEPES (pH 7.9), 0.4 M NaCl, 0.1% Nonidet P-40, 10% v/v glycerol, 1 mM NaF, 1 mM sodium orthovanadate, and a protease inhibitor cocktail (Sigma-Aldrich). Extracts were subjected to SDS-PAGE, followed by blotting onto PVDF membranes. The blots were probed with antibodies of hnRNPA3 (sc-133665), PDIA3 (sc-23886), RAD23B (sc-390019), SYNCRIP/hnRNPQ (sc-56703), LEPRE1 (sc-393003), LIMA1 (sc-136399), MAGOH (sc-271365), p21 (sc-6246), p53 (sc-126), PCNA (sc-56), tubulin (sc-8035) and vinculin (sc-7649) from Santa Cruz Biotechnology (Santa Cruz, CA, USA). Antibody of FLAG M2 was from Sigma-Aldrich.

2.6 Reverse transcriptional and real-time qPCR

Total RNA was extracted with TRIzol Reagent (Invitrogen) and quantified by Nanodrop (Thermo Scientific, Wilmington, DE). RNA preparations were treated with DNase I Amp Grade (Invitrogen) before the cDNAs were synthesized using random primers and iScript cDNA synthesis kit (Bio-Rad Laboratories, Hercules, CA, USA). Transcript levels were quantified using IQ SYBR green Supermix (Bio-Rad) on a CFX96 Real-Time System instrument (Bio-Rad) and primers in different exons of the same gene were designed to detect the levels of mRNAs (Table MM3).

Real-Time qPCRs were performed in triplicate and relative fold changes were calculated using the $2^{-\Delta\Delta C_t}$ method by the formula: $2^{-(\text{sample } \Delta C_t - \text{control } \Delta C_t)}$, where ΔC_t is the difference between the amplification fluorescent thresholds of the gene of interest and the internal reference gene ($\beta 2$ -microglobulin) used for normalization (64).

To detect the expression of mature miR-494, total RNA was extracted with TRIzol reagent, and miR levels were evaluated by using the TaqMan MiRNA Assay kit (Applied Biosystems, Foster City, CA, USA; (28). PCR reactions were performed in triplicate. Small nucleolar RNA RNU6 (Applied Biosystems) was used for

normalization.

Table MM3: Oligonucleotides sequences for RT-qPCR assay

Gene name	Forward primer sequence	Reverse primer sequence
β_2 -microglobulin	5'-CCGTGGCCTTAGCTGTGCT-3'	5'-TCGGATGGATGAAACCCAGA-3'
COL1A1	5'- AAGACGAAGACATCCACCA -3'	5'- AGATCACGTCATCGACAAC -3'
EEF2	5'- GGAGTCGGGAGAGCATATCA -3'	5'- GCACGTTGACTTTCACTG -3'
FUBP1	5'- GACAGTTGATTATACCAAGGCTTG -3'	5'- ATAATCTGGCTGACCACCTGGA -3'
LEPRE1	5'- CGAAGAGATGGAGCTGGAGT -3'	5'- CTTCTGTGGCTGTTCTCT -3'
LEPREL1	5'- AGAGAAGCCAAGCCACACAT -3'	5'- GGCAAGTCCCTCACACAT -3'
LIMA1 α/β	5'- CTGCGTGAATGTCAGAAGA -3'	5'- GCCCAAAGCCTTCATCATAG -3'
MAD1L1	5'- TGGCCTGAGCATCAGGA -3'	5'- TTCAAGGCAAGTCCCTCTG -3'
MAGOHA	5'- TTCAGGCTCGGTTGTCITTT -3'	5'- CAGTTCCTCCATCAGCTTT -3'
MAGOHB	5'- GCGATTCTACTGCGCTAC -3'	5'- GAGGCCACAAAGCATCATCT -3'
MAPRE1	5'- GACGACGAGGCAGCTGAGTT -3'	5'- TTCCTAGCTTCCGAAGTAGAA -3'
XRCC5	5'- CAGGTTCTCAACAGGCTGACTTC -3'	5'- AACTTCTTCTATTGTTTCATGTTGAA -3'

2.7 Senescence-associated β -galactosidase assay

Senescence-associated β -galactosidase (SA- β -gal) activity was assayed according to Dimri et al. (65). Briefly, cells were washed with PBS, fixed with 2% formaldehyde and 0.2% glutaraldehyde in PBS and then equilibrated in PBS. Cells were stained in X-gal staining solution [20 mg/ml X-gal, 40 mM citric acid/sodium phosphate pH 6.0, 5 mM $K_3(FeC_6N_6)$, 5 mM $K_4(FeC_6N_6)$, 150 mM NaCl, and 2 mM $MgCl_2$], at 37 °C, overnight. The percentage of positively stained cells was determined by counting 5 random fields of at least 200 cells each. Images were taken using a Leica AF 6000 (Leica Microsystems, Germany) microscope with Leica Application Suite V4 (LAS V4.1) software.

2.8 Comet assay

The neutral comet assay (Trevigen, Gaithersburg, MD, USA) was carried out according to manufacturer's recommendations. Slides were incubated in lysis buffer for 30 min and in alkaline solution (pH 13) for 40 min; comet tails were generated by 15 min electrophoresis in TBE buffer at 20 V and 4°C. Slides were stained with SYBER Green, and DNA migration was analyzed by fluorescence microscopy (Leica DMS 4000B; Leica Microsystems, Wetzlar, Germany). The tail moment was determined using the Comet assay II software (Perceptive Instruments, Bury St. Edmonds, UK) as described previously (28). A minimum of 100 cells/experiment was analyzed. All the experiments were performed in triplicate.

2.9 Chromatin Immunoprecipitation (ChiP)-qPCR assays

Chromatin Immunoprecipitation (ChiP)-qPCR assays were performed as already described (66), with some modifications. We used three independent biological replicates of IMR90 at PDL34, IMR90 at PDL58 or IMR90 treated with DEM (IMR90-DEM). To cross-link DNA and proteins, formaldehyde was added directly to culture medium (1% v/v final concentration), for 10 min, at room temperature. Then, cells were neutralized with addition of 125 mM glycine, washed three times and scraped into ice-cold PBS. Pellets were resuspended in lysis buffer (1% SDS, 10 mM EDTA, 50 mM Tris-HCl pH 8) supplemented with protease inhibitor cocktail (Sigma). Sonicated chromatin (DNA fragment length of 400 to 1000 bp) was diluted to reach 4 mL into 1% Triton, 2 mM EDTA, 150 mM NaCl, 20 mM Tris-HCl pH 8, protease inhibitor cocktail and quantified. Of these, 400 µg for each sample was stored as DNA input sample or used for Chip-immunoprecipitation with anti-H3K4-me3 or anti-H3K27me3 or normal rabbit IgGs (negative control) antibodies from Millipore (Millipore, Billerica, MA, USA), according to the manufacturer's recommendations. After incubations at 4 °C, overnight, 40 µl of protein A/G Plus-Agarose (sc-2003, Santa Cruz)

were added to each sample and incubation continued for additional 2 h. Chromatin-antibody/protein A/G Plus-Agarose complexes were centrifuged and sequentially washed once with: i) Low Salt Buffer (0.1% SDS, 1% Triton, 2 mM EDTA, 150 mM NaCl, 20 mM Tris-HCl pH 8), ii) High Salt Buffer (Low Salt containing 500 mM NaCl), iii) LiCl Buffer (0.25 M LiCl, 0.5% NP-40, 0.5% Na-deoxycholate, 1 mM EDTA, 10 mM Tris-HCl pH 8), and twice with TE Buffer. DNA and proteins were recovered after their incubation in 1% SDS, 0.1 M NaHCO₃, at 65 °C, for 2 h. Then, NaCl was added to a 10 mM final concentration and protein-DNA cross-links were reversed by incubating samples, at 65 °C, overnight. Samples were digested with proteinase K, at 45 °C, for 1 h. DNA was purified by phenol-chloroform extraction and resuspended in 20 µl for quantification. DNA input sample cross-links were reversed in a similar manner. Real-Time qPCR was performed in triplicate on 1/40 of the immunoprecipitated materials or 1/400 of the input, by using oligos specific for each gene promoter (Table MM4). The relative enrichment of co-immunoprecipitated promoter fragments was determined based on the threshold cycle (Ct) values, as described before (67). Briefly, in the three conditions for each promoter, fold changes of H3K4me3 or H3K27me3 ChIPs relative to control IgGs ChIP were calculated by the following formula: $2^{-\Delta\Delta Ct}$. $\Delta\Delta Ct$ values represent the difference of the ΔCt value obtained after immunoprecipitation with a determined antibody and the ΔCt value for the corresponding sample immunoprecipitated with negative control (rabbit IgGs). In each condition, ΔCt values for specific promoters were determined by subtracting the Ct value of the input from the Ct value obtained in the same sample after immunoprecipitation with the antibodies of interest.

Table MM4: Oligonucleotides sequences for Chip-qPCR assay

LEPRE1-promoter	5'-CCACCGACTCACAATGACAG-3'	5'-CTTTCGGCTCAGACCTCACT-3'
LIMA1 α -promoter	5'-ACTATGGGTGTGCACCACTG -3'	5'-GAGACCAGCCAGACCAACAT -3'
MAGOHA-promoter	5'-GCAGCCAGGCAGAGAATTAC -3'	5'-AGGTGCTGGGAGACGTTAGA -3'
MAGOHB-promoter	5'-TGCCAAAACCTCACAGGCTA -3'	5'-TGACAGTCACCGTCTTTTT -3'

2.10 Statistical analysis

Statistical analyses were carried out using the Student's t-test; data were considered significant at a value of $p \leq 0.05$ (***) or $p \leq 0.01$ (*).

3. Results

3.1 Proteomic analysis by Two Dimensional-Difference Gel Electrophoresis (2D-DIGE) coupled to Mass Spectrometry (MS) and bioinformatic prediction of putative miRNA-494 targets.

A previous study of our laboratory has recently demonstrated that cellular senescence of IMR90 fibroblasts is accompanied by a vast deregulation of microRNA expression. Functional studies demonstrated that among the up-regulated miRNAs, a set of them (miR-210, miR-376a*, miR-486-5p, miR-494, miR-542-5p) promotes the senescence program when transfected in young cells (28). In particular, miR-494 elicit the most robust effects, as demonstrated by induction of specific markers of senescence.

To identify the direct targets of miR-494, we employed a quantitative proteomic strategy based on the consideration that functional miRNA-target interactions lead to reduced levels of proteins derived from the corresponding transcripts.

We carried out a proteomic analysis by 2D-DIGE at 96 h after transfection of miR-494; in these conditions, protein levels of cyclin-dependent kinase 6 (CDK6) and cyclin D1, two known targets of miR-494, were strongly reduced (data not shown). Total protein samples derived from IMR90-miR-scramble and IMR90-miR-494 transfected cells were differentially labeled with Cy3 (green) or Cy5 (red) dyes, mixed and separated by 2D-DIGE.

The DeCyder Differential Analysis Software was used to localize and analyze the protein spots within a gel and also to perform comparative statistical analysis throughout the gels. With this analysis, approximately 2700 protein spots were resolved within a pH 3-10 range and 10-120 kDa molecular mass ranges and of these about 1500 protein spots were matched between the different gels. Among these, the DeCyder analysis reveals that 102 protein spots (38 up- and 64 down-regulated) were differential expressed in miR-494 transfected cells compared to miR-scramble control, with average ratio greater or equal to 1.50 for up- and less than or equal to -1.50 for down-regulated protein spots ($p \leq 0.05$). To automatically pick these up- and down-regulated protein spots, a preparative gel was stained with

SYPRO Ruby (**Figure 3**). Picked spots were digested with trypsin and then analyzed by nanoLC-ESI-LIT-MS/MS (nano-Liquid Chromatography coupled to ElectroSpray-Linear Ion Trap-tandem Mass Spectrometry). This analysis revealed that a total of 172 protein species were present in the deregulated spots due to the occurrence of comigrating proteins in the same spot or of the same protein in more than one spot.

We focused our subsequent analyses on the 121 proteins present in the down-regulated spots, since they could be putative targets of miR-494. Very interesting, among these proteins, BUB3, lamin B1, manganese superoxide dismutase (MnSOD), peroxideroxin-1 (PRDX1) and XRCC5/Ku80 were identified and previously reported as linked to senescence (68-72), thus confirming the validity of our approach.

To search putative direct target of miR-494, we performed *in silico* analysis with 5 different algorithms (TargetScan 6.2, miRDB, miRanda, PITA, and RNA hybrid) on the respective mRNAs of the 121 down-regulated proteins after miR-494 over-expression.

We selected putative targets following two levels of stringency. The first one was based on the intersections of 3 different algorithms, which allow us to select 26 putative targets of miR-494 (**Table 1**). In a second level of stringency, we filtered these 26 putative targets for conservation among mammals and found 7 genes with highly conserved- and 19 with poorly conserved-seed region.

Based on this analysis, we decided to investigate if the 3'UTRs of COG3, EIF5, ENAH, GK, hnRNPA3, RAD23B, and SYNCRIP/hnRNPQ (hereinafter called SYNCRIP) contain functional sites for miR-494. Furthermore, among the remaining putative miR-494 targets having poorly conserved miR-494 binding sites in their 3'UTRs, we selected MAPRE1 and PDIA3 as representative genes because of the high abundance of the corresponding proteins in 2D-DIGE/MS analysis.

Results

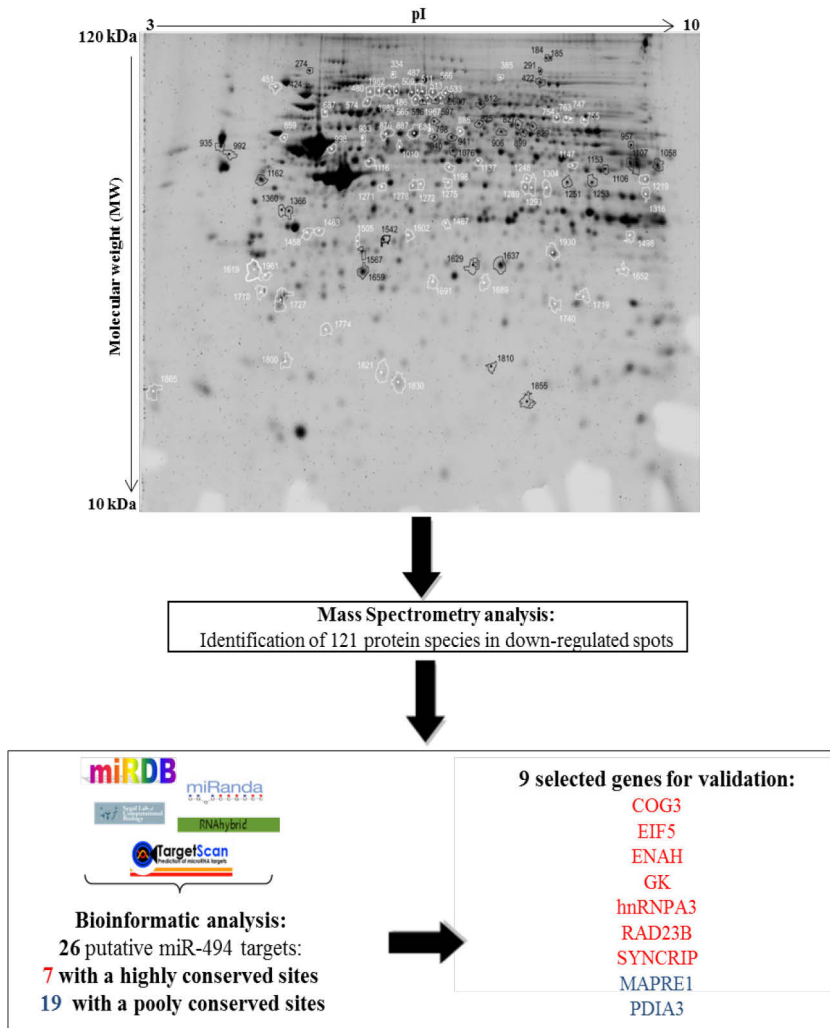


Figure 3

Figure 3: Proteomic strategy based on 2D-DIGE/MS analysis coupled to bioinformatic prediction of miRNA-494 targets. In figure is showed the scan of the preparative gel stained with SYPRO Ruby. The up-represented and down-represented spots are numbered (black and white, respectively).

By bioinformatics tools (TargetScan, miRDB, RNAhybrid, miRanda and PITA) we search for miR-494 potential targets among the transcripts corresponding to the 121 down-regulated proteins. Among the 26 putative miR-494 targets, predicted by at least 3 algorithms, we selected a subset of 9 genes. In this group are included the 7 genes with highly conserved miR-494 sites and 2 with poorly conserved sites, as the latter were high abundant in 2D-DIGE/MS.

Results

Table 1. List of 26 putative miR-494 targets predicted by *in silico* computational analysis.

Gene symbol	Gene name	Accession number*	Target prediction programs	N. conserved/ poorly conserved sites (TargetScan)
<i>ACTR3</i>	<i>Actin-related protein 3</i>	NM_005721	TargetScan, miRanda, PITA, RNA hybrid	0/1
<i>ARPC5</i>	<i>Actin related protein 2/3 complex, subunit 5</i>	NM_005717	TargetScan, miRanda, PITA, RNA hybrid	0/2
<i>CBX1</i>	<i>Chromobox protein homolog 1</i>	NM_006807	TargetScan, PITA, RNA hybrid	0/1
<i>CHCHD3</i>	<i>Coiled-coil-helix-coiled-coil-helix domain containing 3</i>	NM_017812	TargetScan, miRanda, miRDB, PITA	0/1
<i>CNN3</i>	<i>Calponin 3, acidic</i>	NM_001839	TargetScan, miRanda, PITA, RNA hybrid	0/1
<i>COG3</i>	<i>Component of oligomeric golgi complex3</i>	NM_031431	TargetScan, miRanda, PITA, RNA hybrid	1/0
<i>EIF5</i>	<i>Eukaryotic translation initiation factor 5</i>	NM_001969 NM_183004	TargetScan, miRanda, miRDB, PITA, RNA hybrid	1/1
<i>ENAH</i>	<i>Enabled homolog (Drosophila)</i>	NM_001008493 NM_018212	TargetScan, miRanda, miRDB, PITA, RNA hybrid	1/3
<i>FXR1</i>	<i>Fragile X mental retardation syndrome-related protein 1</i>	NM_001013438	TargetScan, miRanda, miRDB, PITA, RNA hybrid	0/2
		NM_005087	TargetScan, miRDB, RNA hybrid	0/2
		NM_00101349		
<i>GK</i>	<i>Glycerol kinase</i>	NM_000167	TargetScan, miRanda, miRDB, PITA	1/3
<i>GLO1</i>	<i>Lactoylglutathione lyase</i>	NM_006708	TargetScan, miRanda, PITA, RNA hybrid	0/1
<i>GOT2</i>	<i>Aspartate aminotransferase, mitochondrial</i>	NM_002080	TargetScan, miRanda, PITA, RNA hybrid	0/1
<i>GRSF1</i>	<i>G-rich sequence factor 1</i>	NM_001098477 NM_002092	TargetScan, PITA, RNA hybrid	0/2

Results

<i>hnRNP A3</i>	<i>Heterogeneous nuclear ribonucleoprotein A3</i>	NM_194247	TargetScan, miRanda, miRDB, PITA, RNA hybrid	1/0
<i>MAPK1</i>	<i>Mitogen-activated protein kinase 1</i>	NM_002745	TargetScan, PITA, RNA hybrid	0/1
<i>MAPRE1</i>	<i>Microtubule-associated protein RP/EB family member 1</i>	NM_012325	TargetScan, PITA, RNA hybrid	0/1
<i>PARVA</i>	<i>Alpha-parvin</i>	NM_018222	TargetScan, PITA, RNA hybrid	0/2
<i>PDIA3</i>	<i>Protein disulfide-isomerase A3</i>	NM_005313	TargetScan, MiRanda, PITA, RNA hybrid	0/1
<i>PGAM1</i>	<i>Phosphoglycerate mutase 1</i>	NM_002629	TargetScan, PITA, RNA hybrid	0/1
<i>PSME3</i>	<i>Proteasome activator complex subunit 3</i>	NM_005789 NM_176863	miRanda, PITA, RNA hybrid	0/0
<i>RAD23B</i>	<i>UV excision repair protein RAD23 homolog B</i>	NM_002874	TargetScan, miRanda, miRDB, PITA, RNA hybrid	1/1
<i>RAI14</i>	<i>Retinoic acid induced 14</i>	NM_015577	TargetScan, miRanda, miRDB, PITA, RNA hybrid	0/3
		NM_001145523	TargetScan, miRanda, miRDB, RNA hybrid	0/3
<i>SRI</i>	<i>Sorcini</i>	NM_198901	TargetScan, miRanda, PITA, RNA hybrid	0/1
<i>STAT1</i>	<i>Signal transducer and activator of transcription 1</i>	NM_007315	TargetScan, miRanda, miRDB, PITA, RNA hybrid	0/3
<i>SYNCRIP/hnRNPQ</i>	<i>Synaptotagmin binding, cytoplasmic RNA interacting protein</i>	NM_006372**	TargetScan, miRanda, miRDB, PITA, RNA hybrid	1/0
		NM_001159673**	TargetScan, miRanda, miRDB, RNA hybrid	2/0
<i>WDFY1</i>	<i>WD repeat and FYVE domain containing 1</i>	NM_020830	TargetScan, miRanda, miRDB, PITA, RNA hybrid	0/2

* Accession numbers correspond to those reported in TargetScan 6.2

** Out of the seven transcript variants, only two are reported that are representative of the two different 3'UTRs of the SYNCRIP mRNAs.

3.2 hnRNPA3, PDIA3, RAD23B and SYNCRIP -3'UTRs are real direct targets of miR-494

The functional studies were performed using constructs containing the regions (200 bp) encompassing the miR-494 recognized sites of the 9 selected genes, cloned downstream of the luciferase genes.

These report plasmids were co-transfected in presence of premiR negative control (miR-SCR) or premiR-494 in IMR90 cells and the luciferase activity was assessed. As shown in **Figure 4A**, over-expression of miR-494 significantly ($p < 0.05$) inhibited the activity of the reporter constructs bearing the wild-type (WT) 3'UTRs of hnRNPA3, RAD23B, SYNCRIP and PDIA3 genes in IMR90 cells when compared with miR-SCR-transfected cells.

To validate these results we also used for each gene, 2 constructs that contain the same regions but in inverted orientation (MUT1) or point-mutations in the binding sites of miR-494 (MUT2). These experiments showed that both mutants abolish the effect of miR-494. These results indicate that hnRNPA3, RAD23B, SYNCRIP and PDIA3 are direct targets of miR-494 in IMR90 cells.

Next, by Western blotting experiments, we examined the endogenous expression of hnRNPA3, RAD23B, SYNCRIP and PDIA3 after miR-494 over-expression in IMR90 cells at PDL33. **Figure 4B** shows that protein levels of above genes were significantly reduced in IMR90 cells expressing high levels of miR-494 when compared with the scrambled control.

Then, to investigate whether the decrease of endogenous miR-494 was able to increase the expression of the above genes, we transfected IMR90 at PDL33 with either a miR-494 inhibitor (anti-sense oligonucleotide ASO-494) or an ASO negative control (ASO-cont). As shown in figure 4B, protein levels of hnRNPA3, RAD23B, SYNCRIP and PDIA3 were up-regulated while RAD23B slightly increased upon ASO-494 transfection. This up-regulation is comparable to that observed for PTEN, a known miR-494 target (data not shown).

Overall, these results demonstrate that hnRNPA3, RAD23B, SYNCRIP and PDIA3 contain functional binding sites for miR-494.

Results

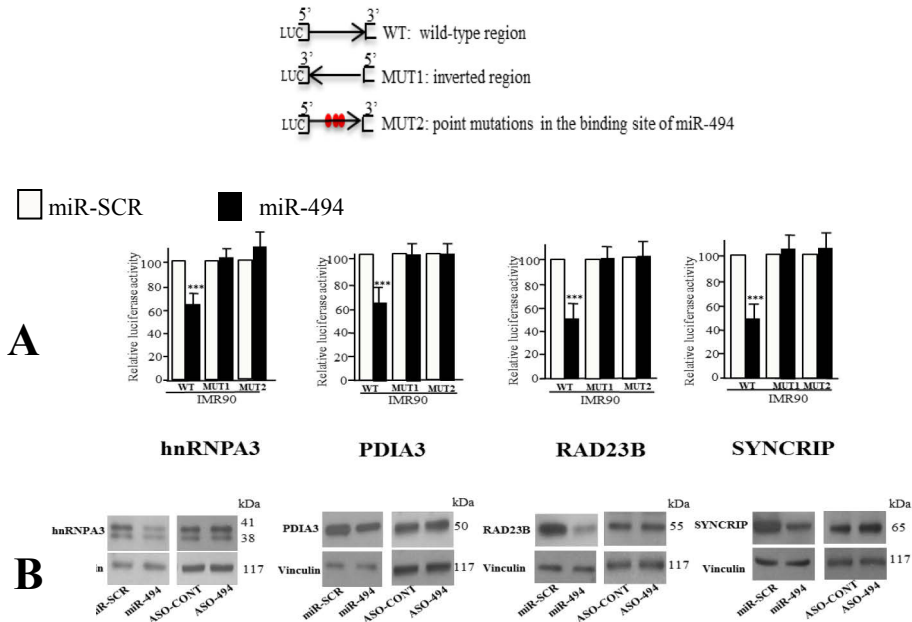


Figure 4

Figure 4: hnRNPA3, PDIA3, RAD23B and SYNCRIP are direct targets of miR-494. A) hnRNPA3, PDIA3, RAD23B and SYNCRIP miR-494 targets were validated by luciferase assay in IMR90 cells. Cells at PDL33 were transfected with luciferase constructs bearing wild-type 3'-UTRs (WT) or inverted (MUT1) or mutated in the seed sequence (MUT2) of miR-494. Cells were also cotransfected with either 100 nM of premiR-494 (miR-494) or premiR negative control (miR-SCR). *Renilla* luciferase was used as an internal control. Triplicate transfection ratio (\pm SD) firefly/*Renilla* luciferase activity were averaged and expressed as percentage of the corresponding transfections with miR-SCR control. *** $p < 0.05$. B) IMR90 cells (PDL33) were electroporated with either negative control (miR-SCR) or premiR-494 (miR-494) and proteins were harvested at 4 d. The same cells were also electroporated with either ASO control (ASO-cont) or ASO-miR-494 (ASO-494) and harvested at 4 d. The protein levels were analyzed by Western blotting experiments. Vinculin was used as a loading control.

3.3 hnRNPA3, PDIA3, RAD23B and SYNCRIP are down-regulated in different models of senescence.

To investigate if downregulation of hnRNPA3, PDIA3, RAD23B and SYNCRIP is a general phenomenon occurring in senescence, we tested expression of these genes in 3 other different senescence models: i) in replicative senescent IMR90 cells at PDL60, ii) in WI38 fibroblasts that are senescent at passage 23 and iii) in stress-induced senescence of IMR90 after chronic DEM treatment (28). In these senescence models, cells showed elevated SA- β -gal-positive staining, increased p53 and p21 protein levels as well as down-regulation of PCNA (data not shown).

As shown in **Figure 5A**, protein levels of hnRNPA3, PDIA3, RAD23B and SYNCRIP are down-regulated in replicative senescent IMR90 cells and as expected, this well correlate with a significant up-regulation of miR-494 levels in the same population.

In replicative senescent WI38 cells (Figure 5A) we obtained a similar down-regulation of the miR-494 putative targets with exception of RAD23B. Also in replicative senescence of WI38, miR-494 levels were significantly increased when compared to young cells.

Lastly, oxidative stress-induced premature senescence in IMR90 cells (Figure 5B) provokes a down-regulation of PDIA3, RAD23B and SYNCRIP proteins and this is accompanied by significantly up-regulation of miR-494 expression.

All together, our data revealed that up-regulation of miR-494 and afterwards down-regulation of its targets, is a general phenomenon in senescence.

Results

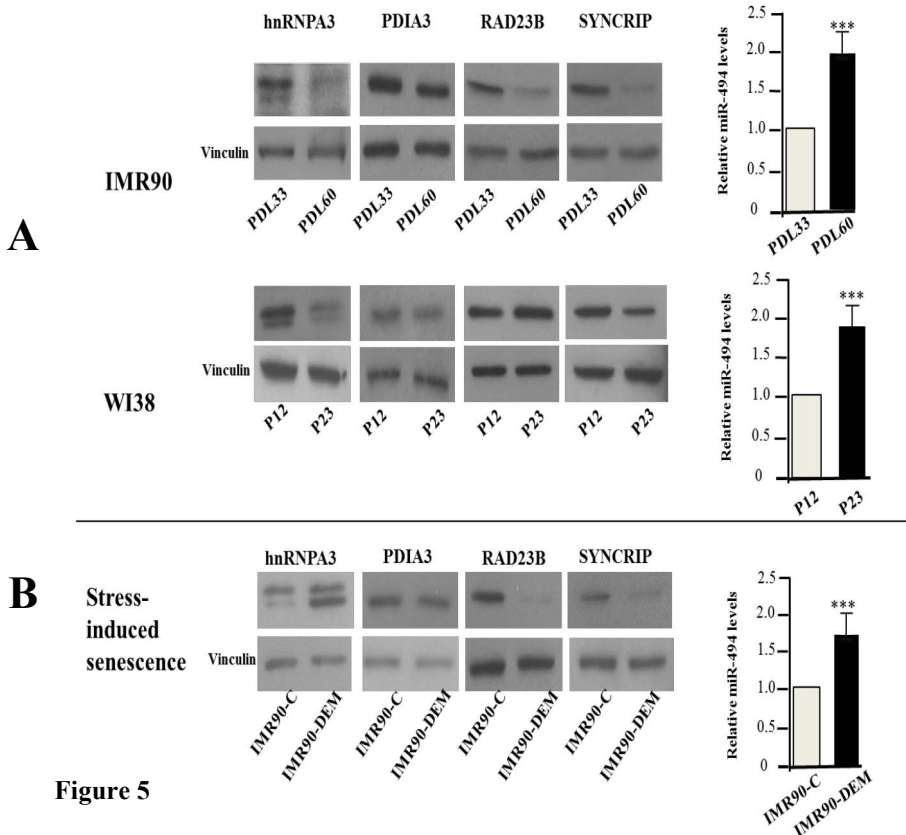


Figure 5: hnRNPA3, PDIA3, RAD23B and SYNCRIP are down-regulated in different models of senescence. A) Western blotting analyses of hnRNPA3, PDIA3, RAD23B and SYNCRIP expression in two models of replicative senescence: IMR90 at PDL 60 and WI38 at passage 23. Vinculin was used as loading control. In the same panel, on the right, the levels of miR-494 in the respective senescent cell populations are reported. miR-494 expression was evaluated by RT-qPCR after normalizing to RNU6 expression and are reported as relative to PDL33-control cells. Columns represent means \pm SD of 3 independent populations. *** $p < 0.05$. B) IMR90 cells at PDL33 were treated with DEM (100 μ M) for 10 d (IMR90-DEM), and protein levels of hnRNPA3, PDIA3, RAD23B, and SYNCRIP were examined by Western blotting. Vinculin was used as a loading control. Analyses of miR-494 expression (right panel), in control (IMR90-C) and DEM-senescent IMR90 cells (IMR90-DEM) were performed as described in B. Columns represent means \pm SD of 3 independent cell populations. *** $p < 0.05$.

3.4 Functional effects of down-regulation of miR-494 targets in young IMR90 cells

To establish whether down-regulation of hnRNPA3, PDIA3, RAD23B and SYNCRIP is causally related to senescence, we silenced them in young IMR90 cells by RNA interference-mediated knockdown (siRNA), and evaluated the appearance of senescent phenotypes by testing specific markers such as cellular proliferation, SA- β -gal activity and DNA damage. Knockdown of PDIA3 cells by siRNA transfection was cytotoxic in young cells; thus, this gene was not further investigated.

Data obtained with the silencing of SYNCRIP have shown that down-regulation of this gene is not causally involved in senescence because no evident markers were detected after siRNA transfection. On the contrary, as shown in **Figure 6A**, downregulation of hnRNPA3 or RAD23B caused a strong reduction in cell growth ($p < 0.05$) in a time-dependent manner, compared with the negative siRNA control. In parallel, we tested the SA- β -gal activity after silencing of hnRNPA3 and RAD23B and the results demonstrate that siRNA-mediated down-regulation of hnRNPA3 or RAD23B caused a robust increase of SA- β -gal activity (Figure 6B). Furthermore, we used neutral comet assay to assess if silencing of hnRNPA3 and RAD23B were able to induce a DNA damage by accumulation of double-strand DNA breaks. Results shown Figure 6C, demonstrate that reduction of hnRNPA3 or RAD23B levels induced accumulation of double-strand DNA breaks when compared with controls. We have used etoposide- and negative siRNA control-treated cells as positive or negative controls, respectively.

Finally, in order to confirm the senescence-like phenotype induced by knockdown of hnRNPA3 and RAD23B, we tested the protein levels of senescence molecular markers such as p53, PCNA and p21. The obtained results showed that p53 and its direct transcriptional target p21 are induced upon siRNA-mediated downregulation of hnRNPA3 or RAD23B.

Overall, these results indicate that hnRNPA3 and RAD23B are effectors of the miR-494-induced senescent phenotype and that

Results

cellular senescence induced either by hnRNPA3 or RAD23B knockdown was associated with up-regulation of p53 and p21 proteins (Figure 6D), a key signaling pathways of senescence onset.

Results

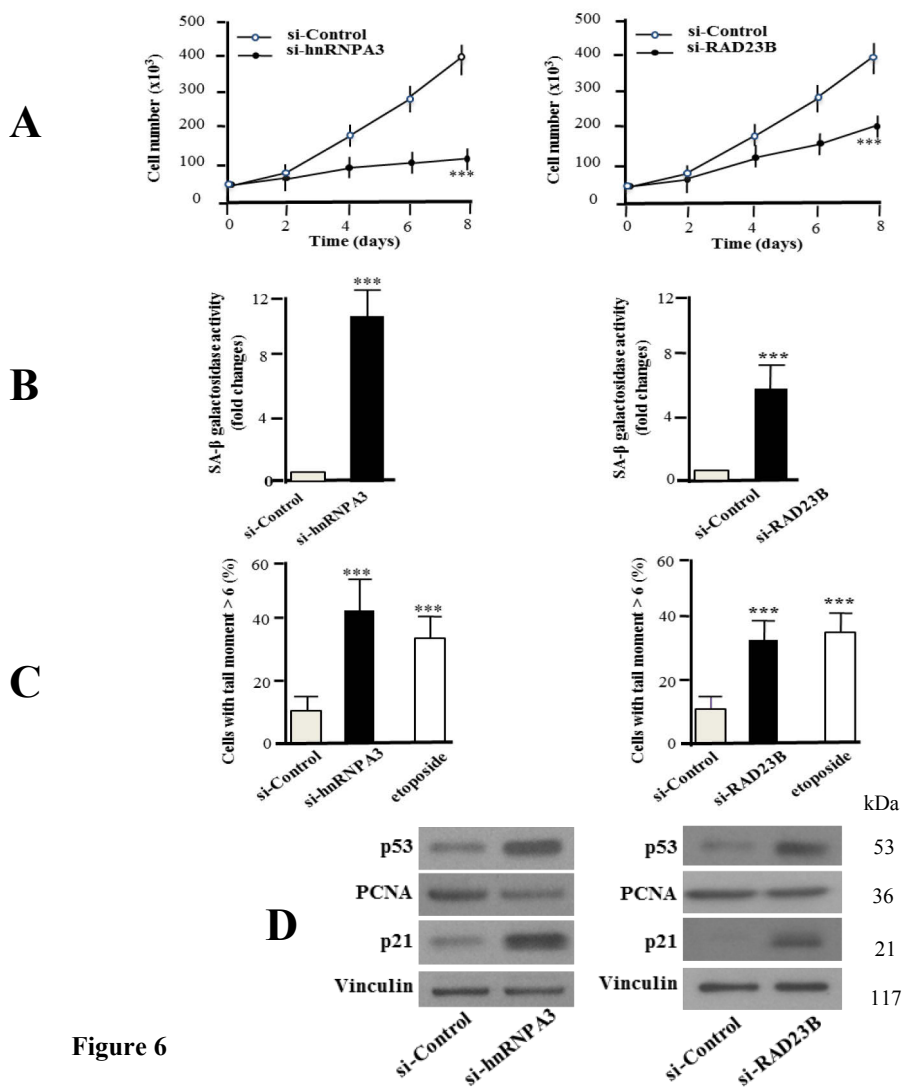


Figure 6

Figure 6: Functional effects of hnRNPA3 and RAD23B down-regulation in young IMR90 cells. A) IMR90 cells at PDL33 were transfected in triplicate with siRNA-negative control or with indicated siRNAs and plated into 6-well plates (50,000 cells/well). Cell counts were performed at indicated time points. Bars represent means \pm SD. *** $p < 0.05$. B) SA- β -gal activity was detected by X-gal staining at 7 d after transfection with siRNAs for hnRNPA3 and RAD23. Counts of ≥ 300 cells were averaged and expressed as fold change \pm SD with respect to the siRNA negative control. *** $p < 0.05$. C) Indicated siRNAs were transfected in PDL33 IMR90 cells. After 4 d, cells were harvested, and comet tails were generated by electrophoresis. Slides were stained with SYBER Green, and DNA migration was analyzed by fluorescence microscopy. Tail moment was determined, and nuclei were divided into 2 classes based on the value of the tail moment. Percentage of damaged cells (tail moment >6) is indicated by the bar graphs. A minimum of 100 cells/experiment was analyzed. *** $p < 0.05$. D) Analyses of the senescence molecular markers p53, PCNA, and p21 proteins by Western blotting were performed at 4 d after transfection of the indicated siRNAs. Vinculin was used as a loading control.

3.5 Role of the miR-494 targets in the senescence program

To establish definitively that hnRNPA3 and RAD23B are real effectors of miR-494-induced senescence we have ectopically expressed these genes individually and verified if this condition was able to delay the senescence triggered by miR-494.

In this experiment young IMR90 cells were first transfected with plasmids driving the expression of hnRNPA3 and RAD23B, lacking 3'UTR, and thus refractory to miR-494, or empty vector, and sequentially transfected with premiR-494.

As shown in **Figure 7**, the ectopic expression of hnRNPA3 or RAD23B slowed the appearance of the senescent phenotype induced by over-expression of miR-494 in young IMR90 cells. In fact, the cell number was significantly increased when the cells were transfected with hnRNPA3 or RAD23B, compared with cells transfected with the empty vector (Figure 7A). These results well correlate with the data of SA-b-gal assay (Figure 7B), where the increase of positive cells was hampered by ectopic expression of hnRNPA3 or RAD23B. Finally, Western blotting experiments showed that this delay is accompanied by reduced protein levels of p53 and p21 (Figure 7C, compare lines 2, 4, and 6).

The results suggest that over-expression of hnRNPA3 or RAD23B slow down the appearance of the markers of senescence induced by miR-494 in young IMR90 cells.

Results

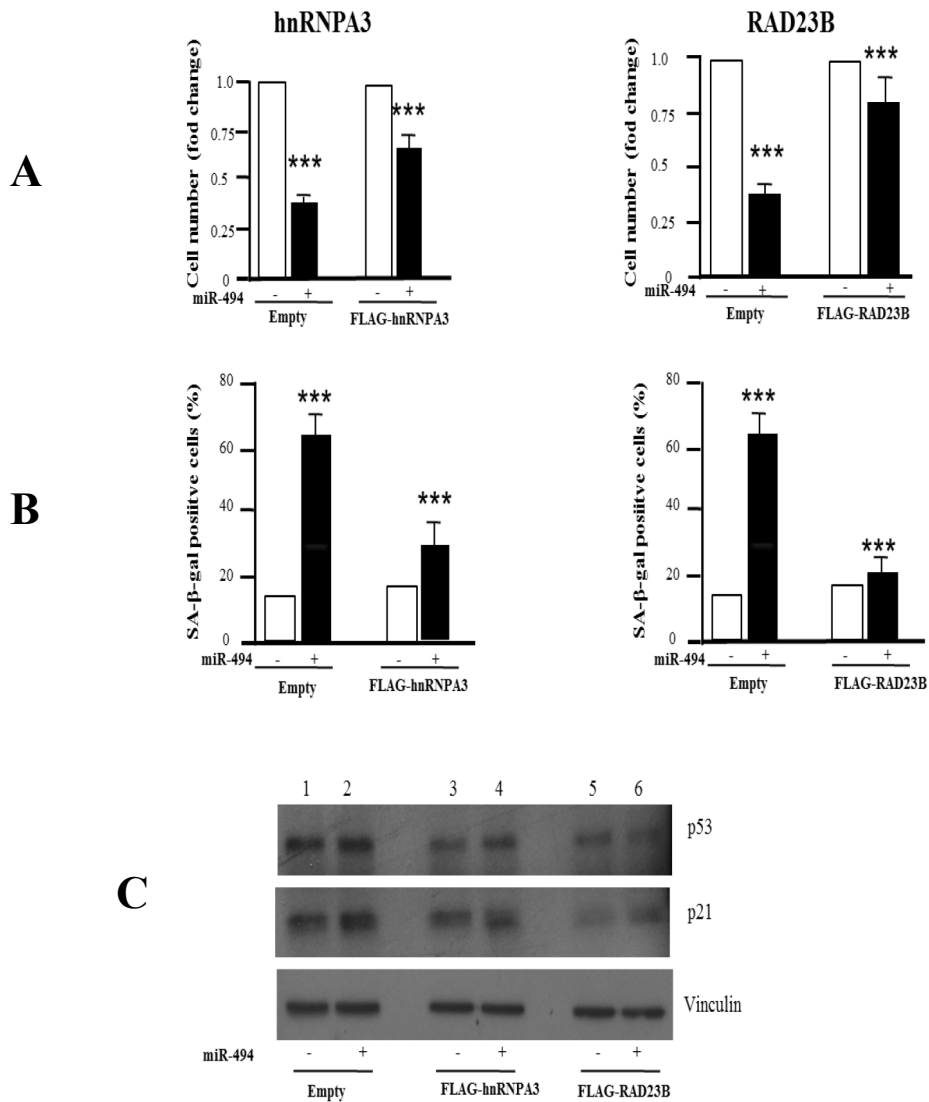


Figure 7

Results

Figure 7: Ectopic expression of hnRNPA3 or RAD23B in young IMR90 cells hampers the senescence process induced by miR-494. A) IMR90 cells at PDL33 were transfected with plasmids driving the expression of either hnRNPA3 or RAD23B, lacking 3'UTRs, or empty vector. After 24 h, the same cells were transfected with 100 nM of premiR-494 (miR-494) or premiR negative control (miR-SCR) for 4 d. Cell numbers were assessed and counts expressed as fold change \pm SD with respect to the negative control. B) SA- β -gal activity was detected by X-gal staining at 7 d after transfection with premiR-494. Counts of ≥ 300 cells were averaged and expressed as fold change \pm SD with respect to the scrambled negative control. C) Western blotting analysis of p53 and p21 was performed at 4 d after transfection with miR-494. Vinculin was used as a loading control. Columns represent means \pm SD of ≥ 3 independent experiments. *** $p < 0.05$.

3.6 Comparative proteomic analysis of IMR90 senescence induced either by telomere shortening or by oxidative stress.

To identify novel genes acting as common mediators of the senescence process in IMR90, we performed comparative differential proteomic analyses based on 2D-DIGE.

We used total protein extracts from cells induced to senescence either by telomere shortening after serial passage *in vitro* (IMR90 at PDL58) or by oxidative stress provoked by chronic mild treatment with the glutathione-depleting agent diethylmaleate (DEM-treated IMR90 cells) and young untreated control cells (IMR90 at PDL34). Approximately 2,500 protein spots were resolved within a pH 3-10 range and 10-120 kDa molecular mass range and about 1,400 valid spots were matched throughout the gels for DeCyder statistical analysis. Following quantitative and statistical analysis and using as selection criteria fold changes ≥ 1.50 for spots up-represented (3 in number) and ≤ -1.50 for spots down-represented (17 in number) and p value ≤ 0.05 , we identified 20 protein spots that were significantly modified in both conditions of senescence (**Figure 8A**).

NanoLC-ESI-LIT-MS/MS analysis on these 20 common deregulated protein spots identified 25 protein species (**Table 2**) due to the occurrence of comigrating proteins in the same spot or of the same protein in more than one spot. Of note, among the up-represented or down-represented identified proteins we found some proteins which have been already associated with senescence, such as vimentin (VIM), cathepsin B (CTSB), collagen alpha-1 (I) chain (COL1A1) and collagen alpha-2 (I) chain (COL1A2), thus validating our approach.

To evaluate whether the identified 25 proteins with altered abundances are also regulated at transcriptional level, total RNA was extracted from three independent cell populations for each condition of senescence and the expression levels of these genes were analyzed by RT-qPCR. As reported in Figure 8B, among the 23 genes encoding for the proteins identified within the down-represented spots, 10 genes, COL1A1, EEF2, FUBP1, LEPRE1, LIMA1, MAD1L1, MAGOHA, MAGOHB, MAPRE1 and XRCC5, were significantly (p

Results

≤ 0.05) down-regulated at least 2 fold at RNA transcriptional levels in both replicative and stress induced-senescence.

Overall these results, demonstrate that replicative and stress-induced senescence share a subset of proteins that are commonly down-regulated and among these more than 50% are also regulated at transcriptional level.

Results

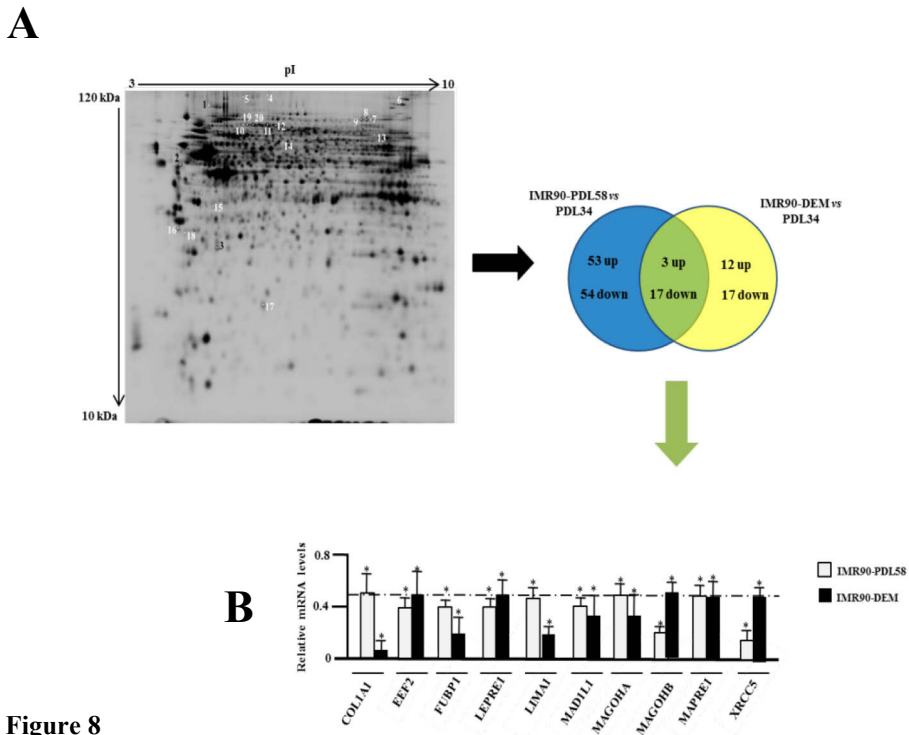


Figure 8

Figure 8: Comparative 2D-DIGE and transcriptional analysis of genes identified in spots common to both conditions of senescence. A) Scan of the analytical, “master” gel of Cy2-labelled protein mixtures from IMR90 at PDL34, replicative IMR90 (PDL58) and DEM-senescent IMR90 cells. In the panel, up- and down-represented protein spots common to replicative- and DEM induced-senescent cells are numbered (black and white color, respectively); numbers correspond to those reported in Table 2. The Venn diagram represents the number of the modified protein spots identified in each condition of senescence and those shared between replicative and DEM-induced senescence. B) mRNA levels encoding for the common genes identified in selected spots of senescent IMR90 cells were analyzed in triplicate by RT-qPCR. The panel reports transcript levels of the genes (10 in number) that were significantly ($p \leq 0.05$) down-regulated at least 2 fold also at RNA transcriptional level in both types of senescence. Relative mRNA levels in senescent cells were calculated by assigning the arbitrary value 1 to the amount observed in young IMR90 cells. The $\beta 2$ -microglobulin transcript level was used as reference. Each column represents the mean \pm SD of 3 independent cell populations; $*p \leq 0.05$. The symbols of the genes correspond to those reported in Table 2.

Results

Table 2. List of the common proteins identified as differentially represented in replicative (PDL58) and DEM-senescent IMR90 cells as revealed by 2D-DIGE and nLC-ESI-LIT-MS/MS analyses. Spot numbering corresponds to that reported in Figure 8A. The statistical significance in differences of protein spots were assessed by the Student's t-test. Protein accession numbers and gene symbols are from NCBI.

Maste r No. (spot)	Protein name	Gene Symbol	Matched peptides	Mascot score	Protein Mr / pI	PDL58 vs PDL34 Average ratio	PDL58 vs PDL34 fold ²	IMR90-DEM vs PDL34 Average ratio	IMR90-DEM vs PDL34 fold ²
1	Vimentin	VIM	21	832	53676/5.06	2.01	0.0075	3.33	0.0028
2	Vimentin	VIM	39	1510	53676/5.06	1.86	0.0075	2.91	0.0046
3	Cathepsin B	CTSB	10	393	38766/5.88	4.99	0.0012	3.77	0.012
4	Collagen alpha-1(I) chain	COL1A1	17	736	139883/5.6	-2.92	0.0084	-2.46	0.0036
5	Collagen alpha-1(I) chain	COL1A1	26	1399	139883/5.6	-2.13	0.013	-2.29	0.036
6	Collagen alpha-2(I) chain	COL1A2	27	1377	129749/9.08	-2.67	0.041	-2.4	0.043
7	Elongation factor 2	EEF2	34	1389	96246/6.41	-1.93	0.027	-1.79	0.016
8	Elongation factor 2	EEF2	41	1656	96246/6.41	-2.27	0.042	-2.17	0.022
9	Elongation factor 2	EEF2	41	1706	96246/6.41	-2.53	0.00052	-1.8	0.025
10	Vacuolar protein sorting-associated protein 35	VPS35	15	700	92447/5.32	-2.22	0.038	-3.14	0.019
	Heat shock protein HSP 90-alpha	HSP90A	6	336	85060/4.94				
	LIM domain and actin-binding protein 1	LIMAI/E PLIN	8	301	85630/6.41				
	Prolyl 3-hydroxylase 1	LEPRE1	6	264	84196/5.05				
11	Mitochondrial inner membrane protein	IMMT	18	870	84026/6.08	-3.01	0.013	-2.83	0.0069
	X-ray repair cross-complementing protein 5	XRCC5	20	815	83222/5.55				
	Procollagen-lysine-2-oxoglutarate 5-dioxygenase 3	PLOD3	13	672	85302/5.69				
	Mitotic spindle assembly checkpoint protein MAD1	MAD1L1	5	175	83301/5.72				
	Niban-like protein 1	NIBL1/FAM129 B	4	164	84598/5.82				
12	LIM domain and actin-binding protein 1	LIMAI/E PLIN	3	153	85630/6.41	-2.45	0.0046	-2.73	0.013
	Mitochondrial inner membrane protein	IMMT	24	1140	84026/6.08				
	Procollagen-lysine-2-oxoglutarate 5-dioxygenase 3	PLOD3	16	826	85302/5.69				
	Signal transducer and activator of transcription 1-alpha/beta	STAT1	7	292	87850/5.74				
	E3 ubiquitin-protein ligase LRSAM1	LRSAM1	5	209	84567/5.7				
13	Far upstream element (FUSE) binding protein 1	FUBP1	14	668	66362/7.12	-1.84	0.015	-1.52	0.026
14	UDP-N-acetylhexosamine pyrophosphorylase	UAP1	3	143	59131/5.92	-1.85	0.037	-1.83	0.014
15	Microtubule-associated protein RP/EB family member 1	MAPRE1	15	555	30151/5.02	-1.66	0.0041	-1.7	0.034
16	Proteasome subunit alpha type-5	PSMA5	11	447	26565/4.74	-2.06	0.00075	-1.87	0.0051
	Tyrosine 3-monoxygenase/tryptophan 5-monoxygenase activation protein zeta polypeptide	YWHAZ	3	87	27899/4.73				
17	Protein mago nashi homolog A	MAGOH A	3	117	17210/5.74	-21.38	3.30E-005	-24.39	3.90E-005
	Protein mago nashi homolog B	MAGOH B	3	117	17276/5.96				
18	Ubiquitin carboxyl-terminal hydrolase isozyme L3	UCHL3	2	109	26337/4.84	-3.71	0.0017	-3.91	0.01
19	X-ray repair cross-complementing protein 5	XRCC5	4	223	83222/5.55	-3.12	0.0045	-3.08	0.014
	LIM domain and actin-binding 1	LIMAI/E PLIN	5	215	76661/5.66				
	Prolyl 3-hydroxylase 2	LEPREL 1	2	72	81846/5.48				
20	Prolyl 3-hydroxylase 2	LEPREL 1	14	648	81846/5.48	-3.23	0.0051	-2.66	0.019
	X-ray repair cross-complementing protein 5	XRCC5	8	378	83222/5.55				
	LIM domain and actin-binding 1	LIMAI/E PLIN	5	214	85630/6.41				
	Niban-like protein 1	NIBL1/FAM129 B	4	183	84598/5.82				

3.7 RNA interference-mediated knockdown of LEPRE1, LIMA1, MAGOHA and MAGOHB induces a senescent phenotype in IMR90 cells.

To investigate whether the down-regulation of COL1A1, EEF2, FUBP1, LEPRE1, LIMA1, MAD1L1, MAGOHA, MAGOHB and MAPRE1 and XRCC5, observed in proteomic analysis and confirmed in RT-qPCR experiments, was causally related to senescence, we analyzed the effects of their individual ectopic silencing in young IMR90 cells. To this aim, we evaluated specific markers of senescence, such as cell proliferation and SA- β -gal activity after their individual down-regulation by siRNAs. As displayed in **Figure 9A**, the down-regulation of LEPRE1, LIMA1, MAGOHA and MAGOHB caused a significant reduction in cell growth ($p \leq 0.05$) at 4 days after transfection, when compared with a negative siRNA control. Furthermore, as shown in Figure 9B, siRNA-mediated knockdown of LEPRE1, LIMA1, MAGOHA and MAGOHB robustly increased the number of SA- β -gal-positive cells, compared to cells transfected with siRNA control.

To further examine at molecular level the senescence response induced by siRNA-mediated down-regulation of the four mentioned genes, we analyzed the protein levels of p53 and p21, two well known markers of senescence. The results indicate that ectopic down-regulation of MAGOHA and MAGOHB led to a concomitant increase of p53 and p21, conversely the down-regulation of LEPRE1 and LIMA1 fosters senescence independently of the p53/p21 pathway (Figure 9C).

All together, these results suggest that down-regulation of LEPRE1, LIMA1, MAGOHA and MAGOHB expression has a causative role in the induction of cellular senescence in primary IMR90 fibroblasts.

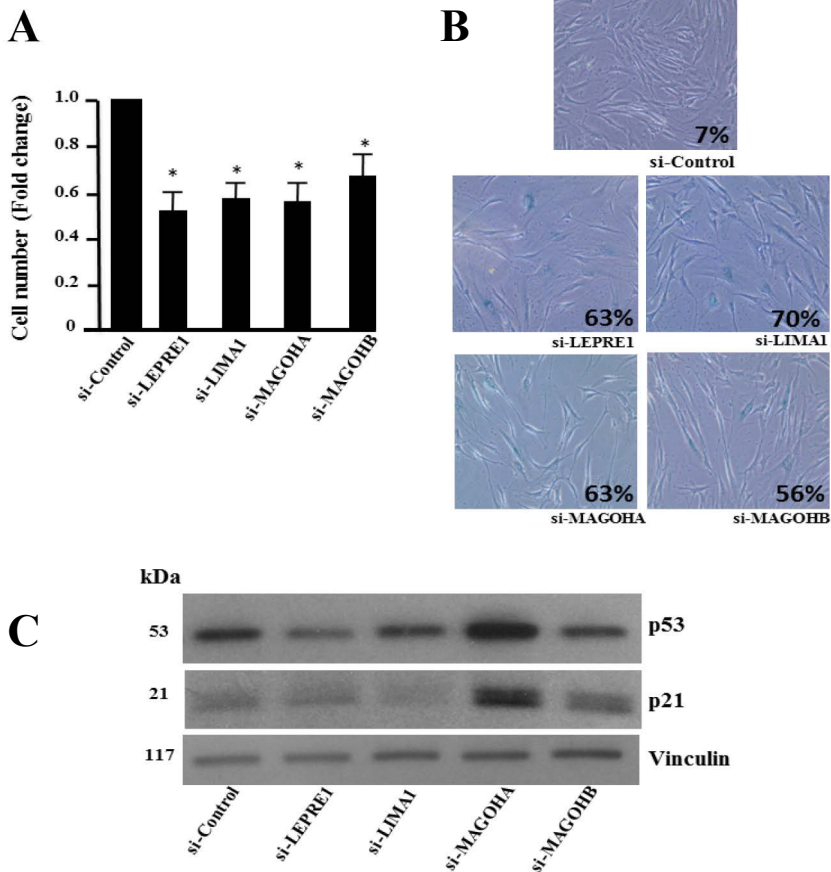


Figure 9

Figure 9: Functional effects of down-regulation of LEPRE1, LIMA1, MAGOHA and MAGOHB in young IMR90 cells. Young IMR90 cells were transfected in triplicate with siRNA negative control or with the indicated siRNAs and plated into six-well plates (50,000 cells/well). Cell counts were performed at 4 d after transfection. Bars indicate means \pm SD. $*p \leq 0.05$. B) SA-β-gal activity was detected by X-gal staining at 7 d after transfection with siRNAs for control and for the indicated genes. The percentage of SA-β-gal-positive cells was calculated by counting ≥ 300 cells and indicated in images. C) Western blotting analysis of p53 and p21 was performed at 4 d after transfection with specific siRNAs. Vinculin was used as a loading control.

3.8 Expression analysis of LEPRE1, LIMA1, MAGOHA and MAGOHB protein in other senescence models *in vitro* and *in vivo*.

To generalize the role of these genes in the senescence process, we analyzed the protein levels of LEPRE1, LIMA1, MAGOHA and MAGOHB in different cellular models of senescence *in vitro* and *in vivo*. For cellular senescence *in vitro*, we used human WI38 primary fibroblasts, in which the senescent phenotype was induced: i) after repeated rounds of replication in culture (reaching at passage 23); ii) prematurely, by treating young cells (p13) with low doses (100 μ M) of DEM for ten days.

In line with the results obtained by proteomic analysis and RT-pPCR (see Figure 8 and Table 2), we confirmed the reduction of the protein levels of LEPRE1, LIMA1, MAGOHA and MAGOHB genes in both condition of senescence, (WI38-p23 and WI38-DEM) (**Figure 10A**). Since MAGOHA and MAGOHB proteins are different only for two amino acid residues in the first four ones, Western blotting analysis displayed only one band with the commercial antibody we used.

To address the *in vivo* relevance of LEPRE1, LIMA1, MAGOHA, and MAGOHB genes in the process of aging, we evaluated their protein expression levels in different cell lines of human fibroblasts from young (age 21–24) or old (age 87–94) subjects (Figure 10B). In these cells the levels of COL1A1 and MMP3 mRNAs are in agreement with that expected for the age of donors (data not shown). The analyses by Western blotting demonstrated a down-representation of protein amounts of the genes mentioned above in cell lines derived from old subjects compared to fibroblasts from young subjects. All together, these results indicate that the protein down-regulation of LEPRE1, LIMA1, MAGOHA and MAGOHB plays a relevant role in senescence process *in vitro* and also highlight an *in vivo* relevance because their expression correlate with human age.

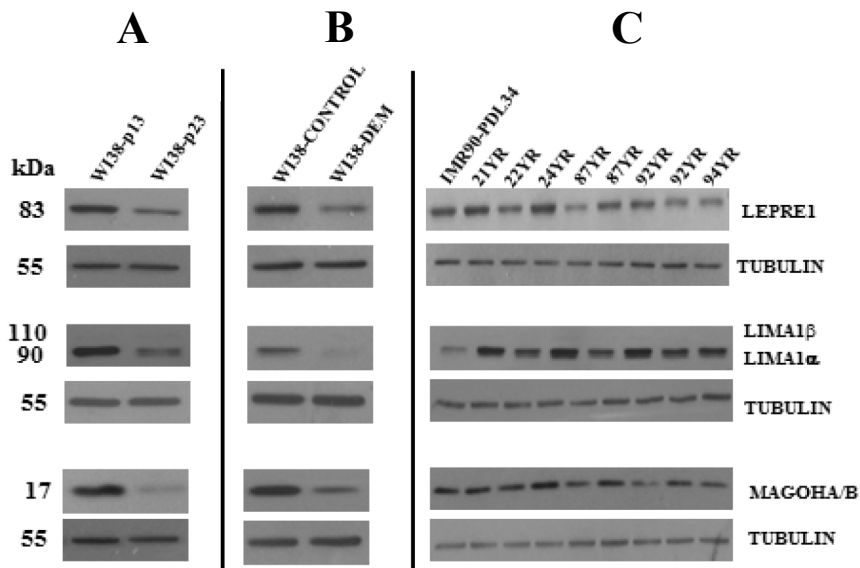


Figure 10

Figure 10: Protein levels of LEPRE1, LIMA1, MAGOHA and MAGOHB in other senescence models. A) Protein amounts of LEPRE1, LIMA1, MAGOHA and MAGOHB in young (p13) and replicative senescent (p23) WI38 cells. B) WI38 untreated cells and cells treated with DEM (100 μ M) for 10 days, were determined by Western blotting experiments. Tubulin was used as a loading control. C) Protein levels of LEPRE1, LIMA1, MAGOHA and MAGOHB in young IMR90 cells and in different cell lines from healthy donors of different ages (indicated in the panels) were determined by Western blotting experiments after two passages in culture. Tubulin was used as a loading control. YR, years.

3.9 H3K4me3 and H3K27me3 changes of the LEPRE1, LIMA1, MAGOHA, and MAGOHB promoters during senescence

To investigate if histone H3 methylation states could affect the observed gene transcription changes of LEPRE1, LIMA1, MAGOHA, and MAGOHB, we performed ChIP-qPCR assays on the promoters of the mentioned genes. In particular, we analyzed the distribution of the trimethylation pattern of histone H3 at Lys4 (H3K4me3), an active mark, and at Lys27 (H3K27me3), a repressive mark, on the region encompassing 500 bp from the start site of these four genes. Analysis was performed on young and replicative- or stress induced-senescent IMR90 cells.

As shown in **Figure 11**, replicative senescent cells display a significant decrease of H3K4me3 in the promoters of LIMA1, MAGOHA, and MAGOHB, when compared to young cells. At the same time, the amounts of H3K27me3 were significantly increased. Our results also show a significant enrichment of H3K27me3 on the promoter of LEPRE1, whereas no changes in H3K4me3 amount were observed on the same region.

In DEM-senescent cells, analysis of local H3K4me3 and H3K27me3 distributions demonstrated that H3K4me3 occupancy on LEPRE1 and LIMA1 promoters was unchanged, but strongly decreased on MAGOHA and MAGOHB promoters. On the contrary, increased recruitment of H3K27me3 was found on the promoter regions of LEPRE1, LIMA1 and MAGOHA genes.

These results suggest that local changes in the H3 methylation states are involved in the reduced expression of LEPRE1, LIMA1, MAGOHA, and MAGOHB genes observed during senescence of IMR90 cells.

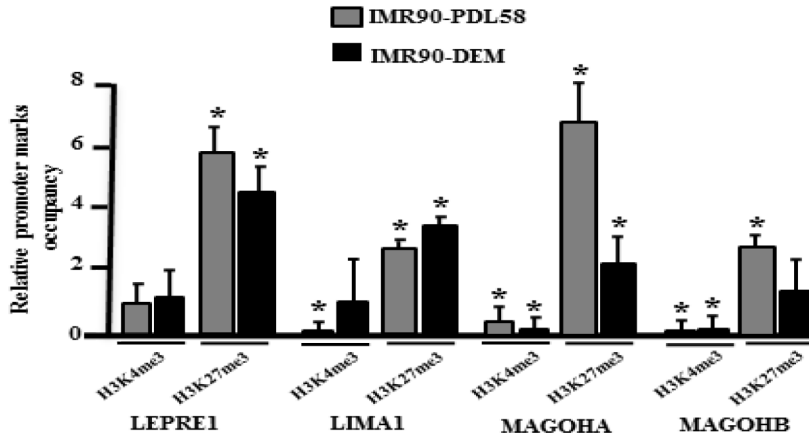


Figure 11

Figure 11: Analysis of H3K4me3 and H3K27me3 states on LEPRE1, LIMA1, MAGOHA and MAGOHB promoters in IMR90 senescent cells. H3K4me3 or H3K27me3 occupancy in the promoter regions (within 500 bp from the start site of the genes) of LEPRE1, LIMA1, MAGOHA and MAGOHB in replicative senescent cells (PDL58) or in young cells treated with DEM (100 μ M) for 10 days were compared to young cells by ChiP-qPCR assays. The relative H3K4me3 or H3K27me3 mark occupancy for each promoter after ChiP was calculated based on the threshold cycle (Ct) values (see Materials and Methods section). Data are expressed by assigning the arbitrary value 1 to the occupancy of the marks observed in young IMR90 cells. Each column represents the mean \pm SD of 3 independent cell populations; * $p \leq 0.05$.

4. Discussion

Molecular program leading to cellular senescence is largely mediated by gene expression changes acting at transcriptional and post-transcriptional levels as well at epigenetic level.

miRNAs regulate gene expression post-transcriptionally by inducing degradation or translation repression of target mRNAs.

In a previous study, we demonstrated that miR-494 is up-regulated in senescent IMR90 human diploid fibroblasts and its ectopic expression in young cells induces premature senescence (28). Therefore, we used a high-throughput proteomic approach to screen for miR-494 targets. The 2D-DIGE coupled to MS let us to identify 121 down-regulated protein species and among these, by functional assays we demonstrated that hnRNPA3, PDIA3, RAD23B and SYNCRIP are direct targets of miR-494. Our results further showed that siRNA-mediated knockdown of hnRNPA3 or RAD23B foster senescence of IMR90 cells. Importantly, we also demonstrated that ectopic expression of hnRNPA3 or RAD23B prevented, at least in part, the senescent phenotype induced by miR-494 in young IMR90 cells.

hnRNPA3 belongs to the hnRNPA/B family, involved in the regulation of the splicing process (73). hnRNPA3 interacts with HuR, another RNA-binding protein involved in cellular senescence (74) and several reports have demonstrated that hnRNPA3 binds to telomeres (75,76). Of note, our data indicate that hnRNPA3 down-regulation is involved in replicative senescence of both IMR90 and WI38 cells, which is triggered by telomere attrition.

RAD23B was characterized as key component of the XPC-nucleotide excision repair (NER) complex. In addition, it is a member of the Oct4/Sox2 transcriptional coactivator complex (77) and is involved in the regulation of ubiquitin-mediated proteolytic process (78) thus affecting a variety of pathways, including stress responses. Therefore, it is plausible that, miR-494-mediated RAD23B down-regulation, negatively affects these functions, thus generating a signal for the senescence program. Of note, in stress-induced senescence, RAD23B is particularly reduced.

The other two direct targets of miR-494 were proved to be PDIA3 and SYNCRIP. For PDIA3, we could not functionally correlate its down-regulation to the senescence program in IMR90 cells, because siRNA experiments resulted in a cytotoxic effect. On the contrary, the results obtained for SYNCRIP demonstrated that its down-regulation by siRNA is not causally involved in the senescence process.

In conclusion, the studies aimed to identify direct targets of miR-494, reveal four novel genes that are post-transcriptionally regulated by this microRNA. Among them, we demonstrated that hnRNPA3 and RAD23B are effectors of the miR-494-induced senescent phenotype and this program involves activation of the p53/p21 pathway. Importantly, the presence of one of them is indeed sufficient to hamper the senescence induced by miR-494.

For the other studies, aimed to identify common regulators of senescence, we also applied the technology of 2D-DIGE coupled to MS analysis. By profiling quantitative proteomic changes occurring both in replicative and stress-induced senescence of human IMR90 fibroblasts, we found that twenty protein spots shifted their quantitative representation in the same direction (over- or down-represented) in both conditions of senescence. Our study also identified proteins, such as vimentin, cathepsin B, COL1A1, COL1A2 and XRCC5/Ku80, which previous proteomic studies in other cellular systems already identified as modified during senescence (79-85). Among the 25 sequence entries obtained from MS analysis, we identified a set of proteins whose decreased representation is associated with the down-regulation of the corresponding mRNAs, thus indicating that the regulation of these genes during senescence occurs at a transcriptional level. Functional studies of 10 genes by siRNAs in IMR90 cells demonstrated, for the first time, that LEPRE1, LIMA1/EPLIN, MAGOHA and MAGOHB genes are causally involved in the induction of cellular senescence.

LEPRE1 is a member of the prolyl 3-hydroxylase family, implicated in the hydroxylation of type I collagen. Inactivation of its gene in mice leads to tendon, skin and bones abnormalities (86), whereas gene mutations are implicated in osteogenesis imperfecta type VIII (87). Very recently, the activity of LEPRE1 as disulfide isomerase has been

reported, thus emphasizing its more general protective function in the cell homeostasis (88).

LIMA1 is a cytoskeleton-associated protein, frequently lost or down-regulated in human cancer (89-91). The fact that siRNA-mediated LIMA1 down-regulation results in premature senescence, may represent a mechanism adopted by normal cells to antagonize the tumor development in pre-cancerous cells, as described for inactivation of other tumor suppressors, such as PTEN, VHL, NF1 and RB, (49,58,92).

MAGOH, Mago-Nashi Homolog, proliferation-associated (*Drosophila*) protein is a component of the core exon junction complex (EJC) (93) involved in splicing, mRNA export, nonsense-mediated mRNA decay (NMD) pathway, and translation initiation (94,95). In humans exist two genes (MAGOHA and MAGOHB) that encode protein isoforms differing only in the first four amino acids (96), indicating that gene redundancy is probably related to an important function of this protein. MAGOH in mice indeed controls brain size by regulating the mRNA levels of LIS1, a master gene for brain development (97). Of note, we found that both MAGOHA and MAGOHB mRNAs are down-regulated in senescence and that siRNA-mediated repression of one isoform is sufficient to drive prematurely senescence involving up-regulation of p53. In fact, as already demonstrated by others in the case of MAGOH mutants (97), our experiments suggest that MAGOH depletion should provoke defective cell division that may result in DNA damage accumulation.

We reported that the expression levels of LEPRE1, LIMA1, MAGOHA, and MAGOHB genes are down-regulated also in other models of senescence *in vitro* (i. e. senescent WI38 cells) and *in vivo* by testing several cell lines of human fibroblasts from young (age 21–24) or old (age 87–94) subjects. These results let to foresee a possible marker role of these genes/proteins in the progression of aging and possibly to follow up age-related conditions.

Considering the role of histone methylation states in transcriptional regulation (14-18, 35-40), we explored *de novo* distribution of H3K4me3 and H3K27me3 at the level of the promoter regions of LEPRE1, LIMA1, MAGOHA, and MAGOHB genes during

Discussion

senescence. We found an increase of the repressive H3K27me3 mark and a significant decrease, in most cases, of active H3K4me3 mark on the promoters of LEPRE1, LIMA1, MAGOHA and MAGOHB gene. This phenomenon well correlated with their decreases at mRNA levels. The role of key enzymes responsible of H3K4 and H3K27 methylation/demethylation changes requires further investigation. In conclusion, we have identified novel proteins, namely hnRNPA3, RAD23B (as direct miR-494 targets), LEPRE1, LIMA1, MAGOHA, and MAGOHB that, being down-regulated in cellular senescence, may represent crucial components of the cellular senescence response.

5. References

- 1). Hayflick, L., Moorhead, P.S. (1961). The serial cultivation of human diploid cell strains. *Exp Cell Res.* 25:585-621.
- 2). Campisi, J., d'Adda di Fagagna, F. (2007). Cellular senescence: when bad things happen to good cells. *Nat Rev Mol Cell Biol.* 8(9):729-40.
- 3). Kuilman, T., Michaloglou, C., Mooi, W.J., Peeper, D.S. (2010). The essence of senescence. *Genes Dev.* 24(22):2463-79.
- 4). Michaloglou, C., Vredeveld, L.C., Soengas, M.S., Denoyelle, C., Kuilman, T., van der Horst, C.M., Majoor, D.M., Shay, J.W., Mooi, W.J., Peeper, D.S. (2005). BRAFE600-associated senescence-like cell cycle arrest of human naevi. *Nature.* 436(7051):720-4.
- 5). Collado, M., Serrano, M. (2010). Senescence in tumours: evidence from mice and humans. *Nat. Rev. Cancer* 10, 51–57.
- 6). Collado, M., Blasco, M. A., Serrano, M. (2007). Cellular senescence in cancer and aging. *Cell* 130, 223–233.
- 7). D'Adda di Fagagna, F. (2008). Living on a break: cellular senescence as a DNA-damage response. *Nat. Rev. Cancer* 8,512–522.
- 8). Campisi, J. (2013.) Aging, cellular senescence, and cancer. *Annu. Rev. Physiol.* 75, 685–705.
- 9). Campisi, J., Robert, L. (2014). Cell senescence: role in aging and age-related diseases. *Interdiscip Top Gerontol.* 39:45-61.
- 10). Itahana, K., Campisi, J., Dimri, G.P. (2007). Methods to detect biomarkers of cellular senescence: the senescence-associated beta-galactosidase assay. *Methods Mol Biol.* 371:21-31.
- 11). Salama, R., Sadaie, M., Hoare, M., Narita, M. (2014). Cellular senescence and its effector programs. *Genes Dev.* 28(2):99-114.
- 12). Muñoz-Espín, D., Serrano, M. (2014). Cellular senescence: from physiology to pathology. *Nat. Rev. Mol. Cell. Biol.* 15(7):482-96.

References

- 13). Fridman, A.L., Tainsky, M.A. (2008) Critical pathways in cellular senescence and immortalization revealed by gene expression profiling. *Oncogene* 27, 5975–5987
- 14). Lanigan, F., Geraghty, J.G., Bracken, A.P. (2011). Transcriptional regulation of cellular senescence. *Oncogene*. 30(26):2901-11.
- 15). Berger, S.L. (2007). The complex language of chromatin regulation during transcription. *Nature*. 447, 407–412.
- 16). Li, B., Carey, M., Workman, J.L. (2007). The role of chromatin during transcription. *Cell*. 128: 707–719.
- 17). Cecco, M., Criscione, S.W., Peckham, E.J., Hillenmeyer, S., Hamm, E.A., Manivannan, J., Peterson, A.L., Kreiling, J.A., Neretti, N., Sedivy, J.M. (2013). Genomes of replicatively senescent cells undergo global epigenetic changes leading to gene silencing and activation of transposable elements. *Aging Cell*. 12:247–256.
- 18). Corpet, A., Stucki, M. (2014). Chromatin maintenance and dynamics in senescence: a spotlight on SAHF formation and the epigenome of senescent cells. *Chromosoma*. 123(5):423-36.
- 19). Naylor, R.M., Baker, D.J., van Deursen, J.M. (2013). Senescent cells: a novel therapeutic target for aging and age-related diseases. *Clin Pharmacol Ther*. 93(1):105-16.
- 20). Brown, C.J., Lain, S., Verma, C.S., Fersht, A.R., Lane, D.P. (2009). Awakening guardian angels: drugging the p53 pathway. *Nat. Rev. Cancer*. 9(12):862-73.
- 21). Chicas, A., Wang, X., Zhang, C., McCurrach, M., Zhao, Z., Mert, O., Dickins, R.A., Narita, M., Zhang, M., Lowe, S.W. (2010). Dissecting the unique role of the retinoblastoma tumor suppressor during cellular senescence. *Cancer Cell*. 17(4):376-87.
- 22). Vernier, M., Bourdeau, V., Gaumont-Leclerc, M.F., Moiseeva, O., Bégin, V., Saad, F., Mes-Masson, A.M., Ferbeyre, G. (2011). Regulation of E2Fs and senescence by PML nuclear bodies. *Genes Dev*. 25(1):41-50.
- 23). Hoare, M., Narita, M. (2013). Transmitting senescence to the cell neighbourhood. *Nat Cell Biol*. 15(8):887-9.

References

- 24). Bartel, D. P. (2009) MicroRNAs: target recognition and regulatory functions. *Cell*. 136, 215–233
- 25). Carthew, R.W., Sontheimer, E.J. (2009). Origins and Mechanisms of miRNAs and siRNAs. *136(4):642-55*. doi: 10.1016/j.cell.2009.01.035.
- 26). Stroynowska-Czerwinska, A., Fiszer, A., Krzyzosiak, W.J. (2014). The panorama of miRNA-mediated mechanisms in mammalian cells. *Cellular and Molecular Life Sciences*. 71(12): 2253-70.
- 27). Stefani, G., Slack, F.J. (2008). Small non-coding RNAs in animal development. *Nat. Rev. Mol. Cell Biol.* 9, 219–230
- 28). Faraonio, R., Salerno, P., Passaro, F., Sedia, C., Iaccio, A., Bellelli, R., Nappi, T. C., Comegna, M., Romano, S., Salvatore, G., Santoro, M., and Cimino, F. (2012). A set of miRNAs participates to the cellular senescence program in human diploid fibroblasts. *Cell Death Differ.* 19, 713–721.
- 29). Gorospe, M., Abdelmohsen, K. (2011). MicroRegulators come of age in senescence. *Trends Genet.* 27, 233–241.
- 30). Mancini, M., Saintigny, G., Mahé C, Annicchiarico-Petruzzelli, M., Melino, G., and Candi, E. (2012). MicroRNA-152 and -181a participate in human dermal fibroblasts senescence acting on cell adhesion and remodeling of the extra-cellular matrix. *Aging (Albany NY)*. 4, 843–853.
- 31). Smith-Vikos, T., and Slack, F. J. (2012). MicroRNAs and their roles in aging. *J. Cell Sci.* 125, 7–17.
- 32). Weilner, S., Schraml, E., Redl, H., Grillari-Voglauer, R., and Grillari, J. (2012). Secretion of microvesicular miRNAs in cellular and organismal aging. *Exp. Gerontol.* 48, 626–633.
- 33). López-Otín, C., Blasco, M.A., Partridge, L., Serrano, M., Kroemer, G. (2013). The hallmarks of aging. *Cell*. 153(6):1194-217.
- 34). Overhoff, M.G., Garbe, J.C., Koh, J., Stampfer, M.R., Beach, D.H., Bishop, C.L. (2014). Cellular senescence mediated by p16INK4A-coupled miRNA pathways. *Nucleic Acids Res.* 42(3):1606-18.
- 35). Narita, M., Nunez, S., Heard, E., Narita, M., Lin, A.W., Hearn, S.A., Spector, D.L., Hannon, G.J., Lowe, S.W. (2003). Rb-mediated heterochromatin

References

formation and silencing of E2F target genes during cellular senescence. 113:703–716.

36). Bracken, A.P., Kleine-Kohlbrecher, D., Dietrich, N., Pasini, D., Gargiulo, G., Beekman, C., Theilgaard-Mönch, K., Minucci, S., Porse, B.T., Marine, J.C., Hansen, K.H., Helin, K. (2007). The Polycomb group proteins bind throughout the INK4A-ARF locus and are disassociated in senescent cells. *Genes Dev* 21: 525–530.

37). Kotake, Y., Cao, R., Viatour, P., Sage, J., Zhang, Y., Xiong, Y. (2007). pRB family proteins are required for H3K27 trimethylation and Polycomb repression complexes binding to and silencing p16INK4alpha tumor suppressor gene. *Genes Dev.* 21: 49–54.

38). Sadaie, M., Salama, R., Carroll, T., Tomimatsu, K., Chandra, T., Young, A.R., Narita, M., Pérez-Mancera, P.A., Bennett, D.C., Chong, H., Kimura, H., Narita, M. (2013). Redistribution of the Lamin B1 genomic binding profile affects rearrangement of heterochromatic domains and SAHF formation during senescence. *Genes Dev.* 27: 1800–1808.

39). Shah, P.P., Donahue, G., Otte, G.L., Capell, B.C., Nelson, D.M., Cao, K., Aggarwala, V., Cruickshanks, H.A., Rai, T.S., McBryan, T., Gregory, B.D., Adams, P.D., Berger, S.L. (2013). Lamin B1 depletion in senescent cells triggers large-scale changes in gene expression and the chromatin landscape. *Genes Dev.* 27:1787–1799.

40). Li, M., Durbin, K.R., Sweet, S.M., Tipton, J.D., Zheng, Y., Kelleher, N.L. (2013). Oncogene Induced Cellular Senescence Elicits an Anti-Warburg Effect. *Proteomics.* 13(17):2585-96.

41). Blasco, M.A. (2005) Telomeres and human disease: ageing, cancer and beyond. *Nat. Rev. Genet.* 6, 611–622.

42). D’Adda di Fagagna, F. (2008) Living on a break: cellular senescence as a DNA-damage response. *Nat. Rev. Cancer.* 8,512–522.

43). Burton, D.G., Krizhanovsky, V. (2014). Physiological and pathological consequences of cellular senescence. *Cell. Mol. Life Sci.* (2014) 71:4373–4386.

44). van Deursen, J.M. (2014). The role of senescent cells in ageing. *Nature.* 509(7501): 439–446.

References

- 45). Shay, J.W., Pereira-Smith, O.M., Wright, W.E. (1991). A role for both RB and p53 in the regulation of human cellular senescence. *Exp Cell Res.* 196: 33–39.
- 46). Ciccia, A., Elledge, S.J. (2010). The DNA damage response: making it safe to play with knives. *Mol Cell.* 40(2):179-204.
- 47). Riley T, Sontag E, Chen P, Levine A. Transcriptional control of human p53-regulated genes. *Nat Rev Mol Cell Biol.* 2008;9:402–412.
- 48). Sikora, E., Arendt, T., Bennett, M., Narita, M. (2011). Impact of cellular senescence signature on ageing research. *Ageing Res Rev.* 10(1):146-52.
- 49). Young, A.P., Schlisio, S., Minamishima, Y.A., Zhang, Q., Li, L., Grisanzio, C., Signoretti, S., Kaelin, W.G. Jr. (2008). VHL loss actuates a HIF-independent senescence programme mediated by Rb and p400. *Nat. Cell Biol.* 10:361–369.
- 50). Lin, H.K., Chen, Z., Wang, G., Nardella, C., Lee, S.W., Chan, C.H., Yang, W.L., Wang, J., Egia, A., Nakayama, K.I., Cordon-Cardo, C., Teruya-Feldstein, J., Pandolfi, P.P. (2010). Skp2 targeting suppresses tumorigenesis by Arf-p53-independent cellular senescence. *Nature* 464:374–379.
- 51). Storer, M., Mas, A., Robert-Moreno, A., Pecoraro, M., Ortells, M.C., Di Giacomo, V., Yosef, R., Pilpel, N., Krizhanovsky, V., Sharpe, J., Keyes, W.M. (2013). Senescence is a developmental mechanism that contributes to embryonic growth and patterning. *Cell.* 155(5):1119-30.
- 52). Muñoz-Espín, D., Cañamero, M., Maraver, A., Gómez-López, G., Contreras, J., Murillo-Cuesta, S., Rodríguez-Baeza, A., Varela-Nieto, I., Ruberte, J., Collado, M., Serrano, M. (2013). Programmed cell senescence during mammalian embryonic development. *Cell.* 155(5):1104-18.
- 53). Kaplon, J., Zheng, L., Meissl, K., Chaneton, B., Selivanov, V.A., Mackay, G., van der Burg, S.H., Verdegaal, E.M., Cascante, M., Shlomi, T., Gottlieb, E., Peeper, D.S. (2013). A key role for mitochondrial gatekeeper pyruvate dehydrogenase in oncogene-induced senescence. *Nature.* 498(7452):109-12.
- 54). Rayess, H., Wang, M.B., Srivatsan, E.S. Cellular senescence and tumor suppressor gene p16.(2012). *Int J Cancer.* 130(8):1715-25.
- 55). Bazarov, A.V., Van Sluis, M., Hines, W.C., Bassett, E., Beliveau, A., Campeau, E., Mukhopadhyay, R., Lee, W.J., Melodyev, S., Zaslavsky, Y., Lee,

References

- L., Rodier, F., Chicas, A., Lowe, S.W., Benhattar, J., Ren, B., Campisi, J., Yaswen, P. (2010). p16^{INK4a} -mediated suppression of telomerase in normal and malignant human breast cells. *Aging Cell*. 9(5):736-46.
- 56). Burton, D.G., Krizhanovsky, V. (2014). Physiological and pathological consequences of cellular senescence. *Cell Mol Life Sci*. 71(22):4373-86.
- 57). Michaloglou, C., Vredeveld, L.C., Soengas, M.S., Denoyelle, C., Kuilman, T., van der Horst, C.M., Majoor, D.M., Shay, J.W., Mooi, W.J., Peeper, D.S. (2005). BRAF^{E600}-associated senescence-like cell cycle arrest of human naevi. *Nature*. 2;436(7051):720-4.
- 58). Chen, Z., Trotman, L.C., Shaffer, D., Lin, H.K., Dotan, Z.A., Niki, M., Koutcher, J.A., Scher, H.I., Ludwig, T., Gerald, W., Cordon-Cardo, C., Pandolfi, P.P. (2005). Crucial role of p53-dependent cellular senescence in suppression of Pten-deficient tumorigenesis. *Nature*. 436(7051):725-30.
- 59). Freund, A., Orjalo, A.V., Desprez, P.Y., Campisi, J. (2010). Inflammatory networks during cellular senescence: causes and consequences. *Trends Mol Med*. 16(5):238-46.
- 60). Scaffidi, P., Misteli, T. (2006). Lamin A-dependent nuclear defects in human aging. *Science*. 312(5776):1059-63.
- 61). Kyng, K.J., May, A., Stevnsner, T., Becker, K.G., Kølvrå, S., Bohr, V.A. (2005). Gene expression responses to DNA damage are altered in human aging and in Werner Syndrome. *Oncogene*. 24(32):5026-42.
- 62). Monteleone, F., Rosa, R., Vitale, M., D'Ambrosio, C., Succio, M., Formisano, L., Nappi, L., Romano, M.F., Scaloni, A., Tortora, G., Bianco, R., Zambrano, N. (2013). Increased anaerobic metabolism is a distinctive signature in a colorectal cancer cellular model of resistance to anti-epidermal growth factor receptor antibody. *Proteomics*. 13(5):866-77.
- 63). Scippa, G.S., Rocco, M., Ialiccio, M., Trupiano, D., Viscosi, V., Di Michele, M., Arena, S., Chiatante, D., Scaloni, A. (2010). The proteome of lentil (*Lens culinaris* Medik.) seeds: discriminating between landraces. *Electrophoresis*. 31, 497–506.
- 64). Livak, K.J., Schmittgen, T.D. (2001). Analysis of relative gene expression data using real-time quantitative PCR and the 2^{-ΔΔC_T} (T). *Method*. 25(4):402-8.

References

- 65). Dimri, G.P., Lee, X., Basile, G., Acosta, M., Scott, G., Roskelley, C., Medrano, E.E., Linskens, M., Rubelj, I., Pereira-Smith, O., Peacocke, M., Campisi, J. (1995). A biomarker that identifies senescent human cells in culture and in aging skin in vivo. *Proc. Natl. Acad. Sci. U. S. A.* 92, 9363–9367.
- 66). Chakrabarti, S.K., James, J.C., Mirmira, R.G. (2002). Quantitative assessment of gene targeting in vitro and in vivo by the pancreatic transcription factor, Pdx1. Importance of chromatin structure in directing promoter binding. *J. Biol. Chem.* 277(15):13286-93.
- j
- 67). Christenson, L.K., Stouffer, R.L., Strauss, J.F. (2001). Quantitative analysis of the hormone-induced hyperacetylation of histone H3 associated with the steroidogenic acute regulatory protein gene promoter. *J. Biol. Chem.* 276, 27392–27399.
- 68) Baker, D. J., Jeganathan, K. B., Malureanu, L., Perez-Terzic, C., Terzic, A., and van Deursen, J. M. (2006) Early aging-associated phenotypes in Bub3/Rae1 haploinsufficient mice. *J. Cell Biol.* 172, 529–540.
- 69). Freund, A., Laberge, R. M., Demaria, M., and Campisi, J. (2012). Lamin B1 loss is a senescence-associated biomarker. *Mol. Biol. Cell.* 23, 2066–2075.
- 70). Velarde, M. C., Flynn, J. M., Day, N. U., Melov, S., and Campisi, J. (2012) Mitochondrial oxidative stress caused by Sod2 deficiency promotes cellular senescence and aging phenotypes in the skin. *Aging* 4, 3–12.
- 71). Turner-Ivey, B, Manevich, Y, Schulte, J, Kistner-Griffin, E, Jezierska-Drutel, A, Liu, Y, and Neumann, C. A. (2013) Role for Prdx1 as a specific sensor in redox-regulated senescence in breast cancer. *Oncogene* 32, 5302–5314.
- 72). Holcomb, V. B., Vogel, H., and Hasty, P. (2007) Deletion of Ku80 causes early aging independent of chronic inflammation and Rag-1-induced DSBs. *Mech. Ageing Dev.* 128, 601–608.
- 73). He, Y., and Smith, R. (2009). Nuclear functions of heterogeneous nuclear ribonucleoproteins A/B. *Cell. Mol. Life Sci.* 66, 1239–1256.
- 74). Yi, J., Chang, N., Liu, X., Guo, G., Xue, L., Tong, T., Gorospe, M., and Wang, W. (2010) Reduced nuclear export of HuR mRNA by HuR is linked to the loss of HuR in replicative senescence. *Nucleic Acids Res.* 38, 1547–1558.

References

- 75). Tanaka, E., Fukuda, H., Nakashima, K., Tsuchiya, N., Seimiya, H., and Nakagama, H. (2007). HnRNP A3 binds to and protects mammalian telomeric repeats in vitro. *Biochem. Biophys. Res. Commun.* 358, 608–614.
- 76). Huang, P. R., Hung, S. C., and Wang, T. C. (2010) Telomeric DNA-binding activities of heterogeneous nuclear ribonucleoprotein A3 in vitro and in vivo. *Biochim. Biophys. Acta* 1803, 1164–1174.
- 77). Fong, Y. W., Inouye, C., Yamaguchi, T., Cattoglio, C., Grubisic, I., and Tjian, R. (2011). A DNA repair complex functions as an Oct4/Sox2 coactivator in embryonic stem cells. *Cell* 147, 120–131.
- 78). Chen, L., and Madura, K. (2002). Rad23 promotes the targeting of proteolytic substrates to the proteasome. *Mol. Cell. Biol.* 22, 4902–4913.
- 79). Nishio, K., Inoue, A. (2005). Senescence-associated alterations of cytoskeleton: Extraordinary production of vimentin that anchors cytoplasmic p53 in senescent human fibroblasts. *Histochem. Cell. Biol.* 123(3):263–273.
- 80). Chrétien, A., Delaive, E., Dieu, M., Demazy, C., Ninane, N., Raes, M., Toussaint, O. (2008). Upregulation of annexin A2 in H(2)O(2)-induced premature senescence as evidenced by 2D-DIGE proteome analysis. *Exp. Gerontol.* 43(4):353-9.
- 81). Aan, G.J., Hairi, H.A., Makpol, S., Rahman, M.A., Karsani, S.A. (2013). Differences in protein changes between stress-induced premature senescence and replicative senescence states. *Electrophoresis.* 34(15):2209-17.
- 82). Keppler, D., Walter, R., Perez, C., Sierra, F. (2000). Increased expression of mature cathepsin B in aging rat liver. *Cell. Tissue Res.* 302:181–188.
- 83). Fisher, G.J., Quan, T., Purohit, T., Shao, Y., Cho, M.K., He, T., Varani, J., Kang, S., Voorhees, J.J. (2009). Collagen fragmentation promotes oxidative stress and elevates matrix metalloproteinase-1 in fibroblasts in aged human skin. *Am. J. Pathol.* 174(1):10114.
- 84). Bigot, N., Beauchef, G., Hervieu, M., Oddos, T., Demoor, M., Boumediene, K., Galéra, P. (2012). NF-κB accumulation associated with COL1A1 transactivators defects during chronological aging represses type I

References

- collagen expression through a -112/-61-bp region of the COL1A1 promoter in human skin fibroblasts. *J. Invest. Dermatol.* 132(10):2360-7.
- 85). Holcomb, V.B., Vogel, H., Hasty, P. (2007). Deletion of Ku80 causes early aging independent of chronic inflammation and Rag-1-induced DSBs. *Mech. Ageing Dev.* 128: 601-608.
- 86). Pokidysheva, E., Zientek, K.D., Ishikawa, Y., Mizuno, K., Vranka, J.A., Montgomery, N.T., Keene, D.R., Kawaguchi, T., Okuyama, K., Bächinger, H.P. (2013). blascotranslational modifications in type I collagen from different tissues extracted from wild type and prolyl 3-hydroxylase 1 null mice. *J. Biol. Chem.* 288(34):24742-52.
- 87). Moul, A., Alladin, A., Navarrete, C., Abdenour, G., Rodriguez, M.M. (2013). Osteogenesis imperfecta due to compound heterozygosity for the LEPRE1 Gene. *Fetal Pediatr Pathol.* 32(5):319-25.
- 88). Ishikawa, Y., Bächinger, H.P. (2013). An additional function of the rough endoplasmic reticulum protein complex prolyl 3-hydroxylase 1·cartilage-associated protein·cyclophilin B: the CXXXC motif reveals disulfide isomerase activity in vitro. *J. Biol. Chem.* 288(44):31437-46.
- 89). Steder, M., Alla, V., Meier, C., Spitschak, A., Pahnke, J., Fürst, K., Kowtharapu, B.S., Engelmann, D., Petigk, J., Egberts, F., Schäd-Trcka, S.G., Gross, G., Nettelbeck, D.M., Niemetz, A., Pützer, B.M. (2013). DNp73 exerts function in metastasis initiation by disconnecting the inhibitory role of EPLIN on IGF1R-AKT/STAT3 signaling. *Cancer Cell.* 24(4):512-27.
- 90). Jiang, W.G., Martin, T.A., Lewis-Russell, J.M., Douglas-Jones, A., Ye, L., Mansel, R.E. (2008). Eplin-alpha expression in human breast cancer, the impact on cellular migration and clinical outcome. *Mol Cancer.* 7:71.
- 91). Zhang, S., Wang, X., Osunkoya, A.O., Iqbal, S., Wang, Y., Chen, Z., Müller, S., Chen, Z., Jossen, S., Coleman, I.M., Nelson, P.S., Wang, Y.A., Wang, R., Shin, D.M., Marshall, F.F., Kucuk, O., Chung, L.W., Zhau, H.E., Wu, D. (2011). EPLIN downregulation promotes epithelial-mesenchymal transition in prostate cancer cells and correlates with clinical lymph node metastasis. *Oncogene.* 30, 4941-4952.
- 92). Nardella, C., Clohessy, J.G., Alimonti, A., Pandolfi, P.P. (2011). Pro-senescence therapy for cancer treatment. *Nat Rev Cancer.* 11(7):503-11.

References

- 93). Bono, F., Gehring, N.H. (2011). Assembly disassembly and recycling: the dynamics of exon junction complexes. *RNA Biol.* 8(1):24-9.
- 94). Le, Hir, H., Gatfield, D., Izaurralde, E., Moore, M.J. (2001). The exon-exon junction complex provides a binding platform for factors involved in mRNA export and nonsense-mediated mRNA decay. *EMBO J.* 20(17): 4987-4997.
- 95). Chazal, P.E., Daguene, E., Wendling, C., Ulryck, N., Tomasetto, C., Sargueil, B., Le Hir, H. (2013). EJC core component MLN51 interacts with eIF3 and activates translation. *Proc. Natl. Acad. Sci. U S A.* 110(15):5903-8.
- 96). Singh, K.K., Wachsmuth, L., Kulozik, A.E., Gehring, N.H. (2013). Two mammalian MAGOH genes contribute to exon junction complex composition and nonsense-mediated decay. *RNA Biol.* 10(8):1291-8.
- 97). Silver, D.L., Watkins-Chow, D.E., Schreck, K.C., Pierfelice, T.J., Larson, D.M., Burnetti, A.J., Liaw, H.J., Myung, K., Walsh, C.A., Gaiano, N., Pavan, W.J. (2010). The exon junction complex component Magoh controls brain size by regulating neural stem cell division. *Nat. Neuroscin.* 13(5): 551-8.